Climate Dynamics (2020) 54:3781–3801
https://doi.org/10.1007/s00382-020-05205-6

Sensitivity studies and comprehensive evaluation of RegCM4.6.1 high-resolution climate simulations over the Tibetan Plateau

Huanghe Gu[1,2] · Zhongbo Yu[1,2] · W. Richard Peltier[3] · Xiaoyan Wang[1]

Received: 12 June 2019 / Accepted: 5 March 2020 / Published online: 17 March 2020

Abstract

This study provides the first comprehensive assessment of Regional Climate Model version 4.6.1 (RegCM4) for the Tibetan Plateau (TP) region. A wide range of model configurations were analyzed with different parameterizations employed to represent cumulus convection (Kuo, Grell, Emanuel, Kain, and Tiedtke), land surface processes (BATS and CLM), planetary boundary layer turbulence (Holtslag and UW PBL), and radiation (CCM3 and RRTM). In addition to the above experiments at a 30-km horizontal resolution, another experiment was conducted based upon the use of a double-nested dynamic downscaling method to construct a simulation at a 10-km resolution to study the sensitivity to the model resolution. We evaluated a 20-year simulation for precipitation, cloud cover, surface radiation budget, 2-m air temperature, and the surface atmospheric circulation against ground and satellite-based observations during the period 1989–2008. Among the factors analyzed regarding sensitivity, precipitation was unsurprisingly found to be sensitive to the cumulus parameterization scheme, and the CLM is found to reduce rainfall compared with BATS, which is satisfactory for both the Emanuel and Tiedtke schemes. Compared with the cumulus convection schemes, the cloud cover and surface radiation budget are sensitive to the land surface, PBL, and radiation schemes. Generally, the CLM is characterized by reduced mean cloud cover and enhanced surface longwave and shortwave radiation compared with BATS. Conversely, the UW PBL and RRTM radiation schemes result in increased cloud cover and less surface radiation compared with the default options in RegCM4. All experiments, except those employing the Kuo scheme, represent the mean 2-m air temperature and regional circulation patterns reasonably well. At the basin scale, the seasonal cycle and interannual variations of precipitation are found to be not well depicted by most model configurations, although the temperature field was well reproduced. Considering all the analyzed variables collectively, the Tiedtke scheme combined with the CLM land surface model is demonstrated to provide the best performance over the TP. However, the higher-resolution version of the model improves the precipitation simulation significantly, particularly in the Brahmaputra river basin, which is located in the north of the Himalayas.

1 Introduction

The Tibetan Plateau (TP), located in central Asia, is the largest and highest plateau on earth, with an average elevation in excess of 4000 m. It has often been referred to as the 'Roof of the World' or the 'Third Pole' of the earth (Qiu 2008; Yao et al. 2019). Moreover, The TP is known for its significant impact on regional and even global climates through the actions of both mechanical and thermal forcing (Nan et al. 2009; Yao et al. 2012). The TP is also referred to as the 'water tower of Asia' because it is the headwater catchment of several major Asian rivers, including the Yellow, Yangtze, Lancang-Mekong, Salween, Ganges–Brahmaputra, and Indus rivers; thus, it supports the environment and livelihood of over 1.4 billion people (Immerzeel et al. 2010). The signature of climate warming in the TP has been apparent over

Electronic supplementary material The online version of this article (https://doi.org/10.1007/s00382-020-05205-6) contains supplementary material, which is available to authorized users.

✉ Huanghe Gu
ghh0001@hhu.edu.cn

✉ Zhongbo Yu
zyu@hhu.edu.cn

[1] State Key Laboratory of Hydrology-Water Resources and Hydraulic Engineering, Hohai University, Nanjing, China

[2] College of Hydrology and Water Resources, Hohai University, Nanjing, China

[3] Department of Physics, University of Toronto, Toronto, Canada

the past half-century, particularly in winter (Guo and Wang 2012; Wang et al. 2008), and the warming trend has been more significant than that at similar latitudes elsewhere (Liu and Chen 2000). Furthermore, this warming has resulted in glacial recession, permafrost degradation, and increases in river discharge and lake levels according to numerous studies (Li et al. 2014, 2017; Wang et al. 2017, 2019a, b; Yang et al. 2010a, b; Yao et al. 2012).

Regional and global climates have changed over the past century, and such changes are expected to continue in the future (IPCC 2013). A series of climate modeling tools have been adopted to investigate and understand the climate over the TP (Gao et al. 2015, 2017; Jiang et al. 2019; Maussion et al. 2011; Shi et al. 2011; You et al. 2018). Owing to their relatively coarse spatial resolution, general circulation models (GCMs) can not usually describe the effects of regional features on the climate adequately (Gu et al. 2015; Jiang et al. 2016; Su et al. 2013; Wang et al. 2018; You et al. 2017; Yu et al. 2018). Meanwhile, regional climate models (RCMs) are able to depict regional heterogeneity and fine-scale forcing (i.e., complex terrain and vegetational variety); thus, they are regarded as the most frequently used tool for basin-scale climate studies (D'Orgeville et al. 2014; Erler and Peltier 2017; Gu et al. 2012; Gula and Peltier 2012; Guo et al. 2018; Peltier et al. 2018; Xu et al. 2005). Previous investigations have suggested that RCMs can reasonably model Asian monsoon climatology and its variability (Gao et al. 2012; Gu et al. 2018; Huo and Peltier 2019; Kim et al. 2008; Oh et al. 2014). Furthermore, RCMs have proven to be effective in enhancing our understanding of the interactions between the surface factors that impact precipitation and the atmospheric system and the effect of external forcing (i.e., sea surface temperature, changes in land surface (Sun et al. 2017)) on the dynamics of the monsoon system (Song et al. 2010; Wang et al. 2016a, b).

Among a dozen of the RCMs currently available (Tapiador et al. 2020), the various versions of RegCM have been some of the most frequently applied to investigate the climate of the TP, as well as many other areas in the world (Ali et al. 2015; Giorgi et al. 2012; Koné et al. 2018; Seth et al. 2007; Sinha et al. 2014; Wang et al. 2013). Moreover, the complexity of RegCM has continued to evolve, with the model version being consistently updated. For example, many aspects were improved in the most recent version released in 2017, including the ability to modify physical parameterizations and the introduction of a new land surface scheme (CLM4.5) to enable the depiction of land surface processes related to land biogeophysics, the hydrologic cycle, biogeochemistry, human dimensions, and ecosystem dynamics. Because many alternative parameterizations can be employed to represent the same physical process in RegCM4, uncertainties are generated in the simulation when the model is applied to any particular region. These uncertainties must be investigated to tune the model to perform optimally in the target region (Huang et al. 2013; Li et al. 2016).

Many sensitivity analyses have been conducted in the context of the work described in this paper to identify a suitable domain size (Almazroui 2015; Dash et al. 2014; Rauscher et al. 2006), adequate horizontal resolution (Gao et al. 2006; Liu et al. 2010), potential driving GCMs (Park et al. 2013), and a physics parameterization scheme (Im et al. 2008; Kang et al. 2014; Wang et al. 2016a, b). When monsoon rainfall is simulated by climate models, the convective parameterization is commonly regarded as the most critical physical process to be accurately represented. In addition, the surface latent heat flux parameterizations over land and the ocean are vital owing to their influence in controlling the quantity of the earth's surface moisture entering the atmosphere (Chen and Avissar 1994; Li et al. 2012). Although a number of scientific reports have confirmed the absence of a best "universal" model setup, improved results have been obtained for certain model configurations under particular climate conditions. However, the current climate models still have limited capability to reproduce the historical climate over the TP. First, the TP is the highest and most extensive highland in the world, with highly heterogeneous terrain and land surface characteristics. Moreover, the TP has a unique planetary boundary layer (PBL), which is approximately 9 km above the sea level, much higher than the surrounding lowlands (Chen et al. 2016). Thus, it is difficult for climate models to properly treat the complex surface heterogeneity and critical processes such as glacier/snow cover–related albedo feedbacks (Su et al. 2013). Meanwhile, the mechanical and thermodynamic forces over the TP are influenced by the Asian monsoon systems, which presents a challenge for current state-of-the-art climate models to simulate (Song and Zhou 2013; Sperber et al. 2013). The work described in the present paper is devoted to investigating a wide range of model configurations as a first step toward the creation of an appropriate ensemble of integrations of the global warming process targeted on the TP.

Therefore, this study is similar in design to many of the above-referenced RCM investigations with the primary novelty being the work focused on the TP region. RCMs have been widely used in regional climate studies over the TP, and remarkably encouraging results have been achieved (Gao et al. 2011; Maussion et al. 2014; Wang et al. 2013, 2016a, b). Xu et al. (2018) and Lin et al. (2018) investigated the impact of the model resolution on precipitation simulation and water vapor transport over the TP by the REMO and WRF models, individually. The results indicate the importance of a higher resolution in precipitation simulation over a complex terrain region. Jiang et al. (2019) evaluated the simulations of summer rainfall over the TP by the WRF model with two horizontal resolutions and two

cumulus schemes. The sensitivity of the RegCM simulations to the land surface models on the TP was studied by Wang et al. (2014). In contrast to previous studies that concentrated on the impact of a single configuration of physical parameterizations applied to modeling the climate at 20–50 km horizontal resolutions for a period of 5–10 years (Ali et al. 2015; Ji and Kang 2013; Shi et al. 2018; Wang et al. 2014; Xu et al. 2018; Zhang et al. 2015), this study was conducted at a finer (10 km) horizontal resolution for a 20-year-period as a basis to evaluate the performance of the climate model with different parameterization schemes. For this purpose, we also selected the source regions of five large rivers as subregions, and validated the model specifically upon these different river basins. The reasons for the selection the TP region as the study area include the following: (a) the TP region is a known "hotspot" that has significantly attracted the interest of national decision-makers; (b) a series of problems continue to exist for the TP when attempts at climate model validation have been conducted; (c) there is a lack of knowledge concerning the temporal and spatial variations of the climate over the TP, which play an important role in studies of terrestrial ecosystems and hydrological processes, as well as a need to further explore the impact of the TP on the Asian monsoon climate.

This article is organized as follows. Descriptions of the climate model to be employed and its most relevant parameterization schemes, as well as the data employed and the experimental design are provided in Sect. 2. In Sect. 3, the results of the performed simulations are presented together with a discussion of their implications. A summary of our conclusions is offered in Sect. 4.

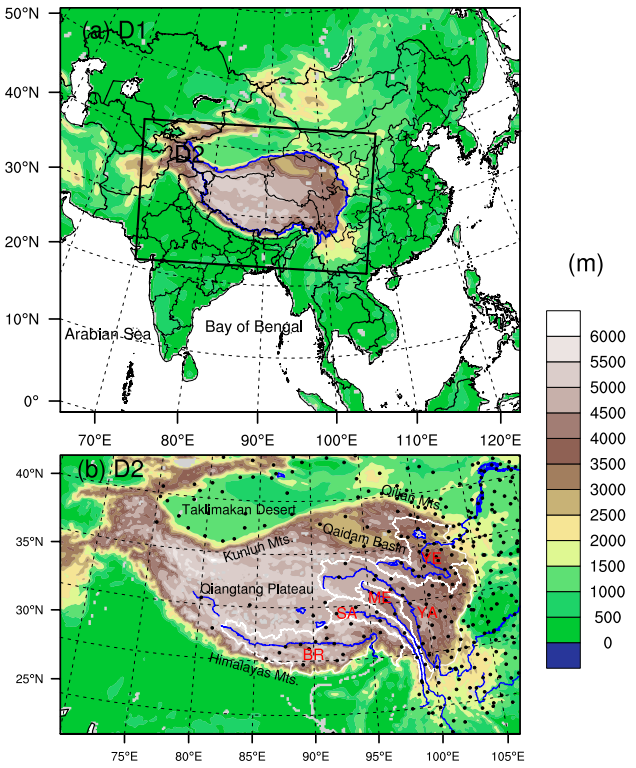

Fig. 1 Domain configurations of the nested RegCM simulations with **a** D1: 30-km resolution and **b** D2: 10-km resolution and the Tibetan Plateau investigation area. The black dots indicate the monitoring stations used to construct the observational reference. The boundaries of the five source river basins are shown in **b** (*YE* Yellow River, *YA* Yangtze River, *ME* Mekong River, *SA* Salween River, *BR* Brahmaputra River)

2 Study area, data, model, and experiments

2.1 Study area

The TP covers five provinces of China (Xizang, Qinghai, Gansu, southern Xinjiang, and western Sichuan) and occupies the region bounded by 25–40° N latitude and 75–105° E longitude (Fig. 1). The TP is famous for its large number of contributing mountain ranges, such as the Kunlun Mountains in the north, the Tangula Mountains in the central region, and the Himalayas on the southernmost margin. The elevation in the TP decreases gradually from the northwest to the southeast, with a mean altitude of 4292 m. Vegetation types include forest, temperate shrubland/meadow, temperate/alpine desert, and ice/polar desert (Cui and Graf 2009).

As previously mentioned, five major river basins situated on the TP were selected as foci for the purpose of the study, namely the upper reaches of the Yellow River (YE), Yangtze River (YA), Mekong River (ME), Salween River (SA), and the Brahmaputra River (BR) (Fig. 1). These five basins display a wide variety of climate, topography, land cover, and hydrological regimes. The Indian monsoon, East Asian monsoon, and the mid-latitude westerlies are critical factors impacting the climate in these basins (Yang et al. 2014; Yao et al. 2012). The annual mean precipitation increases as the elevation diminishes, with more than 70% of the precipitation occurring in the months from May to September.

2.2 Regional climate model (RegCM)

RegCM version 4.6.1 (RegCM4) from ICTP (Giorgi et al. 2012) was applied in this study. It includes the latest non-hydrostatic version and a dynamical core resembling that of the "parent" hydrostatic version of MM5. The physical parameterizations in RegCM4 comprise the moisture scheme at the sub-grid scale (Pal et al. 2007), the radiation package (RAD) of the National Center for Atmospheric Research (NCAR) community climate model version 3 (CCM3) (Kiehl et al. 1996) and the Rapid Radiation Transfer Model (RRTM) (Mlawer et al. 1997), the non-local PBL scheme developed by Holtslag and Boville (1993) and the new University of Washington PBL (UW PBL) scheme (Bretherton

et al. 2004; Grenier and Bretherton 2001), as well as several optional cumulus parameterizations such as the Kuo (Anthes 1977), Grell (Grell 1993), Emanuel (Emanuel 1991), Kain-Fritsch (Kain and Fritsch 1993), and Tiedtke (Kain and Fritsch 1993) schemes, ocean surface schemes (Zeng et al. 1998), and land surface schemes (BATS (Dickinson et al. 1993) and CLM4.5 (Oleson et al. 2008)).

In this study, 6 hourly ERA-Interim reanalysis datasets, which show better performance than other reanalysis data over the TP, with the spatial resolution of $1.5° \times 1.5°$ were applied as the initial and boundary conditions to the climate model (Wang and Zeng 2012). The Optimum Interpolation Sea Surface Temperature is another type of forcing data for the RCM, which constitutes weekly timescale data obtained from the National Oceanic and Atmospheric Administration.

2.3 Observational datasets

The daily precipitation and 2-m air temperature dataset with the spatial resolution of 0.1° (1979–2015) was obtained from the Data Assimilation and Modeling Center of the Institute of Tibetan Plateau Research, Chinese Academy of Sciences (Wang and Zeng 2012). The precipitation data were generated by merging the station observations (Fig. 1; 95 stations located in and 34 stations located on the edge of the TP region) from the China Meteorological Administration with other sources of precipitation data such as the Princeton forcing data, Global Land Data Assimilation System (GLDAS) data, and Tropical Rainfall Measuring Mission (TRMM) satellite precipitation data. The applicability and reliability of the dataset have been verified in other studies (Liu et al. 2019; Wang et al. 2019a, b; Xie et al. 2017). Furthermore, these datasets have been used for land surface water and energy modeling in the TP (Xue et al. 2013) and compared with in situ observation data (Xie et al. 2017).

The monthly satellite-based total cloud cover data from 1983 to 2009 (Rossow and Schiffer 1999), with a native resolution of 2.5°, from the International Satellite Cloud Climatology Project (ISCCP) was employed to evaluate the RCM simulations. In addition, Lange et al. (2015) indicated that the uncertainty from the satellite observations mentioned above reached approximately 5%.

The monthly surface shortwave and longwave net radiation observations on a 1° grid extending from July 1983 to December 2007, developed by Stackhouse et al. (2011) was employed to evaluate the quality of our model simulations. Moreover, Lange et al. (2015) found that the uncertainties for the above shortwave and longwave radiations are 20 W/m^2 and 5 W/m^2, respectively. In addition, the ERA-Interim reanalysis data were selected as the reference data to serve as a basis for our investigation of the performance of the model in terms of wind circulation at 500 hPa.

2.4 Experimental setup

This study focused on the evaluation of climate model simulations over the TP based on different combinations of cumulus parameterization, land surface, PBL, and RAD schemes. First, five options for the cumulus convection scheme were considered: Kuo, Grell, Emanuel, Kain, and Tiedtke. The Kuo scheme, which is the simplest cumulus convection scheme (Giorgi et al. 2012), has been available since the earliest version of RegCM. The Emanuel is the most complex scheme used for depicting the cumulus process, and includes processes such as cloud mixing and ice processes. For the land surface model, CLM4.5 is a more sophisticated model than BATS; the former includes more elaborate surface characteristics, with more soil and snow layers, and uses explicit treatments for both liquid water and ice (Steiner et al. 2009). Meanwhile, the UW PBL and the RRTM are both newly implemented optional schemes in RegCM.

In contrast to other studies, we focused on the sensitivity of RegCM4 with a large number of different configurations, including the combinations of five convection schemes, two land surface models, two PBL schemes, and two radiation schemes. The modeling experiments compromised the current computing resources. Therefore, the convection scheme, which is the most sensitive scheme for precipitation, was treated as the primary calibration scheme. Then, the best convection scheme was selected and used to calibrate the other physical schemes individually. This study included analyses of a total of nine combinations of physical parameterizations to further evaluate the performance of RegCM4. As summarized in Table 1, C1–5 share the same land surface physics, RAD, and PBL schemes to quantify the impact of the cumulus parameterizations. C5 and C6 share the same cumulus, RAD, and PBL schemes, aimed at identifying the effects of two different land surface models, etc. Additionally, C7, C8, and C9 were compared with C5 to test the model sensitivity to the RAD, PBL, and resolution, respectively.

For the experiments listed in Table 1 (except the last experiment), the center of the model grid was fixed at 31° N, 94° E, with 250 grid points along each longitudinal circle and 220 grid points along each latitude direction. The buffer zone at the outer boundaries of the model wass set to be 12 grid points deep with exponential relaxation toward the model forcing and nudging decreasing in strength toward the interior of RegCM. The model was first employed with a horizontal resolution of 30 km and 18 vertical levels (from the surface up to 10 hPa). The study period covered 20 years, ranging from 1989 to 2008, as previously stated. In addition, 1988 was selected as a spin-up period to allow for a full year of equilibration.

Table 1 Nine conducted experiments with five different cumulus parameterization schemes, two radiation schemes, two PBL schemes, two land surface models, and two spatial resolutions

	Acronym	Cumulus parameterization	Radiation scheme	PBL scheme	Land surface model	Resolution (km)
C1	Kuo	Kuo	CCM3	Holtslag	BATS	30
C2	Gre	Grell	CCM3	Holtslag	BATS	30
C3	Ema	Emanuel	CCM3	Holtslag	BATS	30
C4	Kai	Kain	CCM3	Holtslag	BATS	30
C5	Tie	Tiedtke	CCM3	Holtslag	BATS	30
C6	Tie-C	Tiedtke	CCM3	Holtslag	CLM4.5	30
C7	Tie-C-R	Tiedtke	RRTM	Holtslag	CLM4.5	30
C8	Tie-C-P	Tiedtke	CCM3	UW PBL	CLM4.5	30
C9	Tie-C-10	Tiedtke	CCM3	Holtslag	CLM4.5	10

The final experiment in the set to be described employed a double-nested dynamic downscaling method to simulate the climate cover the whole TP at a 10-km resolution with 380 grid points in the longitudinal direction and 232 grids in the latitudinal direction. The 10-km resolution simulation was run within the 30-km resolution domain and used similar physical configurations as those in the C6 experiment. Figure 1b shows the double-nested model domain of C9. A comparison of the two domains demonstrates that the topography is much more highly resolved in the innermost domain at 10-km resolution than in the outermost domain at 30-km resolution (Fig. 1).

Several commonly used statistical measures were employed to quantify the performance of the RegCM4 simulations (Samouly et al. 2018): absolute bias, relative bias, spatial correlation coefficient, and root mean square error.

3 Results

We first analyzed the ability of RegCM4 to simulate the seasonal distributions of precipitation, total cloud cover (TCC), 2-m air temperature, surface shortwave and longwave net radiations, and the wind field at 500 hPa. Next, our analyses focused on the climate of the five river basins considering both the seasonal cycles and interannual variability. Finally, we considered the distribution of the daily precipitation intensities computed using the different RegCM configurations.

3.1 Seasonal climatology

3.1.1 Precipitation

We commence with a discussion of the most important atmospheric variable as far as this study is concerned. The mean precipitations during winter [December–January–February (DJF)] and summer [June–July–August (JJA)] are displayed in Fig. 2. In JJA, the precipitation exhibits a strong southeast-northwest gradient in the rainfall pattern, with the rainfall decreasing from the southeast (rainfall > 5 mm/day) to the northwest (rainfall < 1 mm/day) due to the impact of the Asian summer monsoon in the southern regions. All the model simulations can reproduce these primary precipitation features, but considerable differences exist between the different parameterization schemes. Summarizing a few statistical measures for all five convection schemes (Table S.1), the biases of the mean summer precipitation simulations range from − 1.3 to 91% over the TP for the period 1989–2008. There is a common overestimate of the summer precipitation for all convection schemes, except for a 1.3% underestimate from the Kain scheme. The Kuo scheme overestimates the summer precipitation in the western TP and underestimates the precipitation in the eastern TP. Similarly, the Grell and Kain schemes overestimate the summer precipitation in the northern TP and underestimate the precipitation in the middle and southern TP. As a result, the Kuo, Grell, and Kain schemes exhibit the lowest spatial correlation coefficient (i.e., < 0.3), even though they are characterized by lower average relative biases in summer precipitation. In contrast, the Emanuel and Tiedtke schemes show a higher spatial correlation coefficient, although they significantly overestimate the rainfall compared with observations. As we know, different convection schemes have different physical hypotheses. The Emanuel scheme focuses on the local atmospheric stability, while the Tiedtke scheme focuses on the large-scale water vapor movement (Zhang et al. 2015). The Emanuel scheme is more active in transporting humid air from low levels to high levels, generating more precipitation (Ali et al. 2015). We believe for a thicker PBL, the unique characteristics of deep convection and entrainment in the Tiedtke scheme are responsible for the wet bias reduction in summer precipitation. Considering the above, it is not yet possible to infer a "best" convection scheme based on the ability of the parameterization to reproduce the multi-year mean precipitation.

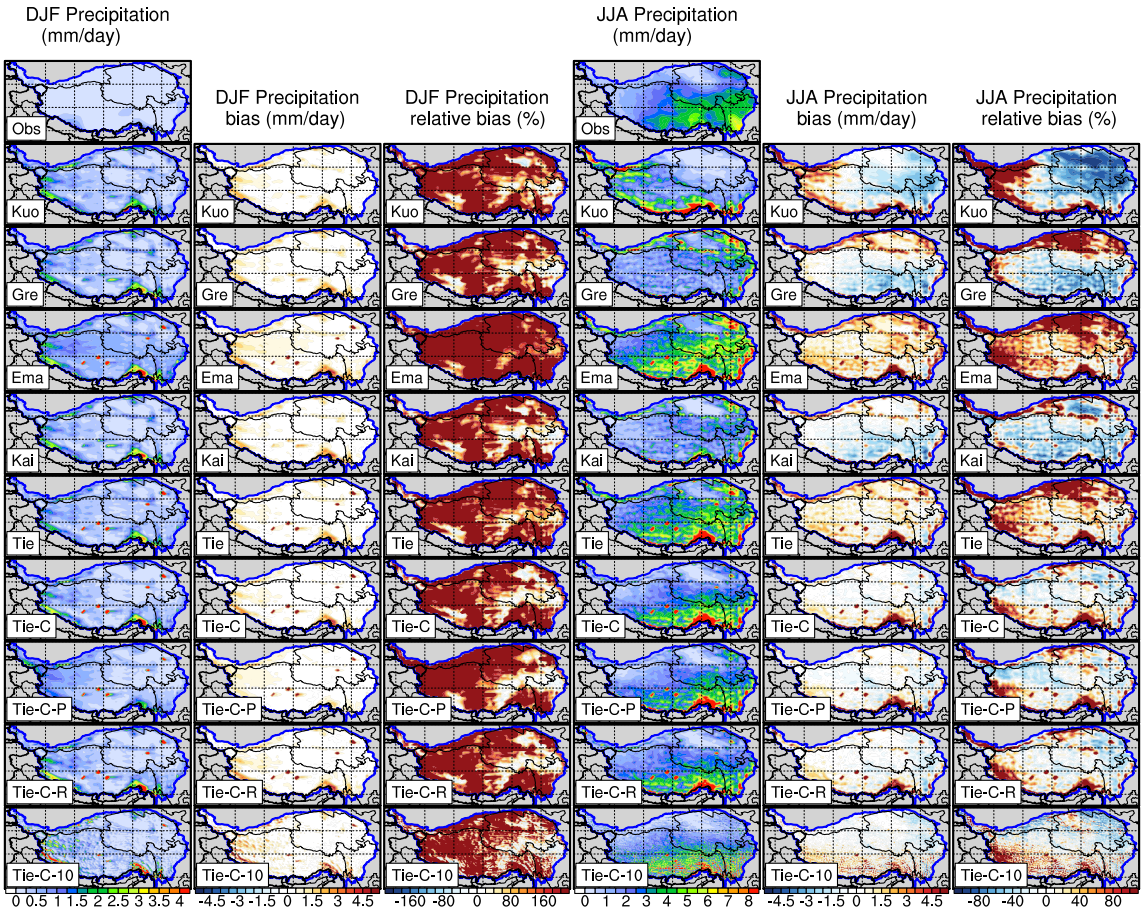

Fig. 2 Observed mean precipitation and simulations for winter (DJF, three leftmost columns) and summer (JJA, three rightmost columns) during the years 1989–2008. For each season, the left column shows the seasonal mean value, while the middle and right columns show the absolute and the relative differences between the observation (topmost row) and the model simulations (from top to bottom), respectively. Here, the model setups (from top to bottom) have been defined in Table 1

Based on the evidence from previous studies, the precipitation amount is expected to be considerably reduced when using CLM to replace BATS as the land surface scheme (Gao et al. 2016). More specifically, the combination of the Emanuel and Tiedtke schemes with the CLM reduces the positive results, which is not the case for other convective schemes when applied over the TP. Similar findings were reinforced by additional simulations using the CLM as the land surface model. The Emanuel and Tiedtke schemes combined with BATS overestimate the summer precipitation by 2.30 and 1.68 mm/day, respectively, while the summer precipitation biases were reduced to 1.36 and 0.97 mm/day, respectively, when combined with CLM. In addition, the overestimations are primarily in the western and southern parts of the TP, where the observations are limited. Considering that the CLM is one of the state-of-the-art land surface models, with possibly the most-advanced parametrizations, it is recommended to be used for areas with complex land surface condition like the TP (Wang et al. 2014). Therefore, the Tiedtke scheme combined with the CLM is suggested to be the preferred convection scheme for annual average precipitation simulations over the TP.

Compared with the convection scheme and land surface model, the PBL parameterizations and radiation schemes have little effect on precipitation. To further investigate the impact of a horizontal resolution on a historical climate simulation, a nested experiment at 10-km resolution was performed. The summer precipitation overestimation at this higher resolution was reduced to 0.43 mm/day. This shows that the higher resolution model performs significantly better at reproducing the magnitude and distribution of historical precipitation.

The winter is characterized by very low precipitation rates (<0.5 mm/day) over most regions of the TP based on observation. The winter precipitation is higher over the Himalayas, in particular in the western and eastern parts, where it can reach more than 2 mm/day. Most simulations could reproduce the above spatial pattern. However, all models consistently overestimate the winter precipitation to be approximately 3 times higher than that observed. This is

consistent with the previous studies, which indicated that higher winter precipitation is commonly estimated in this region with RCM (Dimri and Niyogi 2013; Gao et al. 2015; Ji and Kang 2013; Maussion et al. 2014; Ménégoz et al. 2013). Winter precipitation is not sensitive to the cumulus parameterization scheme and model resolution, implying that it is mainly non-convective. It is also important to note that most winter precipitation occurs in the form of snow. Thus, this overestimation in the winter precipitation will simulate larger snow cover extent and snow depth, which will impact the radiation budget because of the albedo changes (Guo et al. 2019). In turn, this will encourage 2-m air temperature cooling by subsequently reducing the net shortwave radiation (Rangwala and Miller 2012).

3.1.2 Total cloud cover

Clouds play a significant role in the water and energy balance of the atmosphere. The winter and summer mean values of the TCC fractions are shown in Fig. 3. Generally, most models overestimate the winter TCC and underestimate the summer TCC over the TP. In JJA, all the convection schemes show similar results and reproduce the TCC well, with an areal average bias of less than 8% compared with the ISCCP observation data, excluding the Kuo scheme, which underestimates the TCC by approximately 11%. In DJF, all models overestimate the TCC in the north and west parts of the TP and underestimate the TCC in the southeast part of the TP, although an areal average bias of less than 4% was found. In general, the Emanuel and Tiedtke schemes exhibit better performances in reproducing the TCC in magnitude and spatial distribution.

Compared with the convection schemes, a change of land surface model results in larger TCC changes. Generally, the CLM land surface model yields less mean cloud cover of the TP compared with the BATS scheme, although it will partially offset the overestimation in winter. In contrast, the UW PBL parameterization and RRTM radiation scheme tend to yield more cloud cover compared with their default options. Compared with the 30-km simulations, the higher 10-km resolution model has little effect on the model performance in reproducing the TCC over the TP.

3.1.3 Surface shortwave net radiation

Figure 4 shows the spatial distribution of the simulated and observed surface net SW radiations (SW net) for the whole sky. The SW net in winter is much lower than that in summer, and shows a clear decreasing gradient from south to north over the TP. However, the highest SW net was found in the western region of the TP in summer due to the low rainfall and cloud cover in this area. Overall, the model underestimates the SW net, resulting in less solar absorption at the land surface compared to the satellite observations with a bias of approximately -37 to -70 W/m^2 in the summer and winter. A negative bias is widely distributed throughout the entire domain, particularly over the western TP. Regarding the spatial variability, the Tiedtke scheme shows the most realistic spatial distribution of the SW net ($R=0.72$ and 0.73 in summer and winter, respectively). Unlike the TCC, the CLM yields a higher SW net value in summer compared with the BATS scheme, which has a positive impact by reducing the bias. As reported from several previous studies, this anti-correlation between the SW net and TCC biases is physically rational considering the reflection effect of clouds (García-Díez et al. 2015; Pessacg et al. 2014).

3.1.4 Surface longwave net radiation

Figure 5 shows the spatial distribution of the surface net LW radiation for the whole sky. The LW net has a similar magnitude and spatial distribution in winter and summer. The highest LW net was found over the Qaidam basin in the north TP. Regarding the absolute LW, the model clearly underestimates the observations and is not sensitive to the employed parameterization scheme to represent cumulus convection. However, using the CLM instead of the BATS land surface model significantly reduces the summer biases from more than 20 W/m^2 in BATS to less than 4 W/m^2 in CLM. This implies that the CLM land surface model generally increases the outgoing longwave radiation. Overall, the Tiedtke scheme combined with the CLM has the best performance in simulating longwave radiation.

3.1.5 2-m air temperature

The DJF and JJA mean values of the 2-m air temperature, which are related to the surface radiation budget as well as to precipitation, are shown in Fig. 6. Most experiments can reproduce the observed seasonal mean 2-m air temperature over the TP very well, in terms of its spatial distribution. Moreover, the effects of topography on the surface air temperature can clearly be identified in both the observation and model simulations; the surface air temperature is warm in low-altitude areas such as the Qaidam basin and cold in high-altitude areas such as the south and west TP. Furthermore, there is a pronounced cold bias in both winter and summer, particularly in the western and southern TP. In addition, there is a significant warm bias over the northern TP in winter. This finding is in accordance with the results of Wang (2014), whose results were obtained using RegCM4 and the Grell convective scheme coupled with either the BATS or CLM over the TP. Moreover, the cold biases in the model simulations are partially due to the systematic bias in the ERA forcing data (Bao and Zhang 2012; Wang and Zeng 2012). The observations

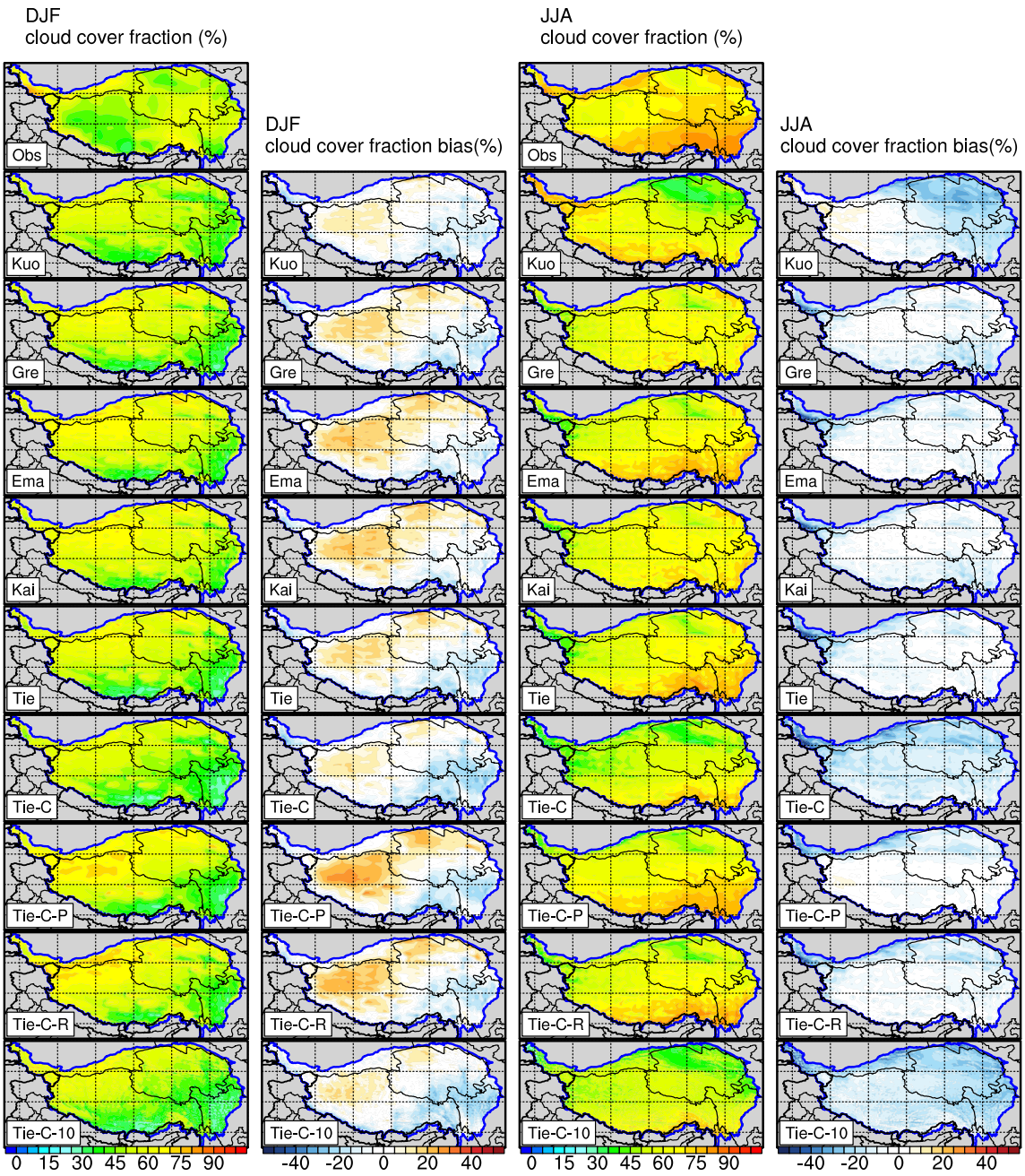

Fig. 3 Mean cloud cover fraction versus observations during winter (DJF, two leftmost columns) and summer (JJA, two rightmost columns) from 1989 to 2008. For each season, the left column shows the seasonal mean value, and the right column presents the absolute difference between the observation (topmost row) and the model simulations (from top to bottom) with the different configurations defined in Table 1

may also have warm bias because the meteorological stations mostly lie in valleys (Gu et al. 2012; Qin et al. 2009). Similarly, the cold biases in the simulations are most probably a direct result of the lack of observations in the western TP and high-latitude areas. In general, the Tiedtke scheme combined with the CLM shows the best performance in simulating the 2-m air temperatures. Contrary to some expectations, the double-nested 10-km resolution simulation tends to overestimate the surface temperature over the eastern TP, particularly in summer.

3.1.6 Regional circulation patterns

It is also important to study the large-scale atmospheric circulation variations when investigating regional climate variations (Zhang et al. 2018). Hence, the model

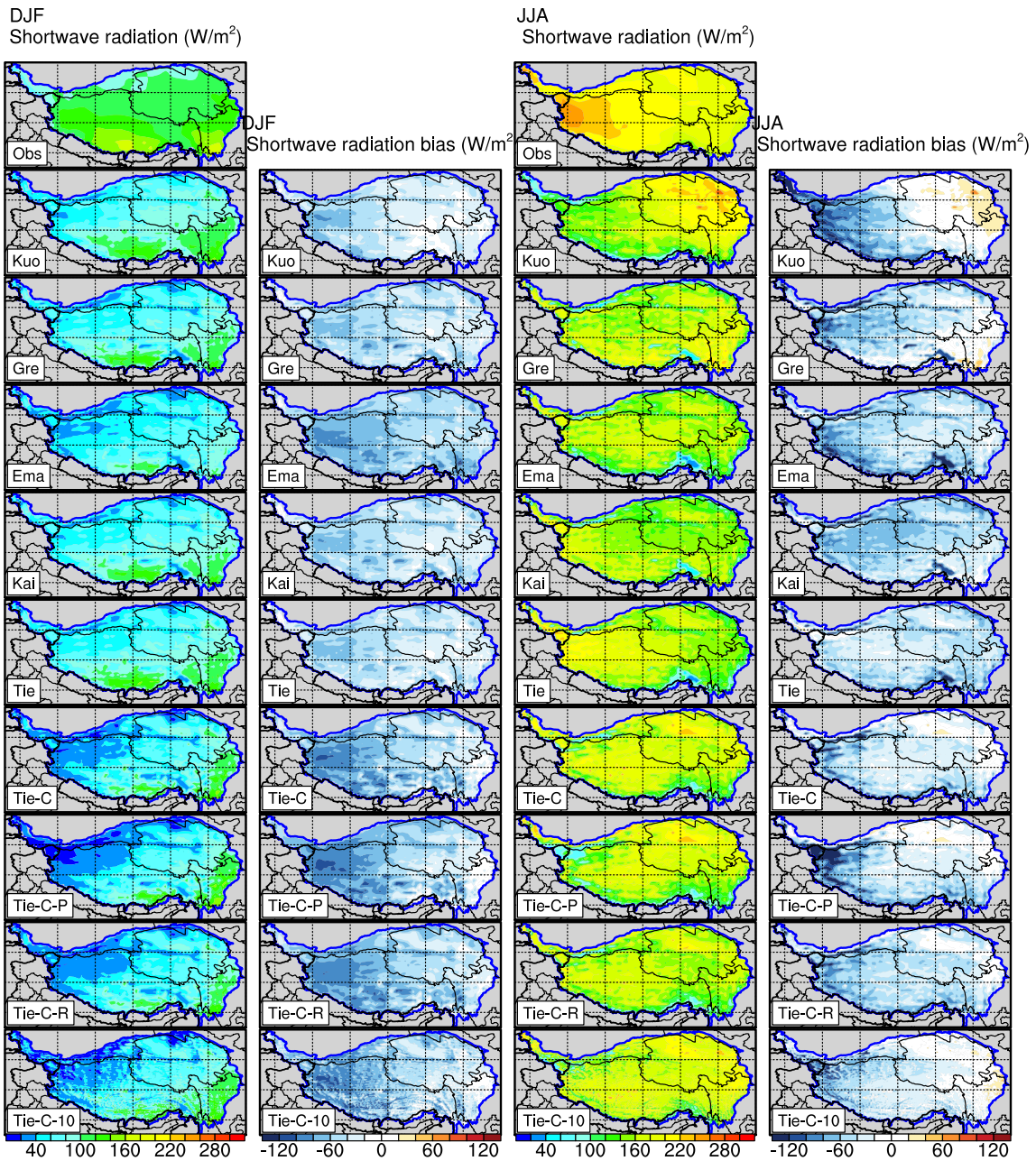

Fig. 4 Same as Fig. 3, but for surface net SW radiation

simulations are further analyzed herein with respect to the circulation characteristics by comparing our model results with the ERA Interim reanalysis. Unlike much of China, the mean sea level pressure is not a suitable field to use for studying the prevailing circulation characteristics over the land surface of the TP due to the high elevation of this region. Considering that the mean elevation of the TP area in this study is higher than 4200 m, and therefore that the 500-hPa level is just above the surface of the TP (Zhang et al. 2018), the 500-hPa wind field was employed for the purpose of analysis in this study.

Figure 7 shows a comparison of the spatial distribution of the 500-hPa wind field circulation obtained in our simulations with the results of the ERA-interim reanalysis for the JJA period. All models except the Kuo convection scheme depict the circulation pattern reasonably well; i.e., the mid-latitude westerlies split into two branches near the western TP in summer, and the moisture is transported from the Arabian Sea and the Bay of Bengal onto the southeastern TP by the Indian summer monsoon. As can be seen in Fig. 7, the Grell and Kain schemes show a stronger westerly flow of air in the northern TP; whereas, the Emanuel and Tiedtke

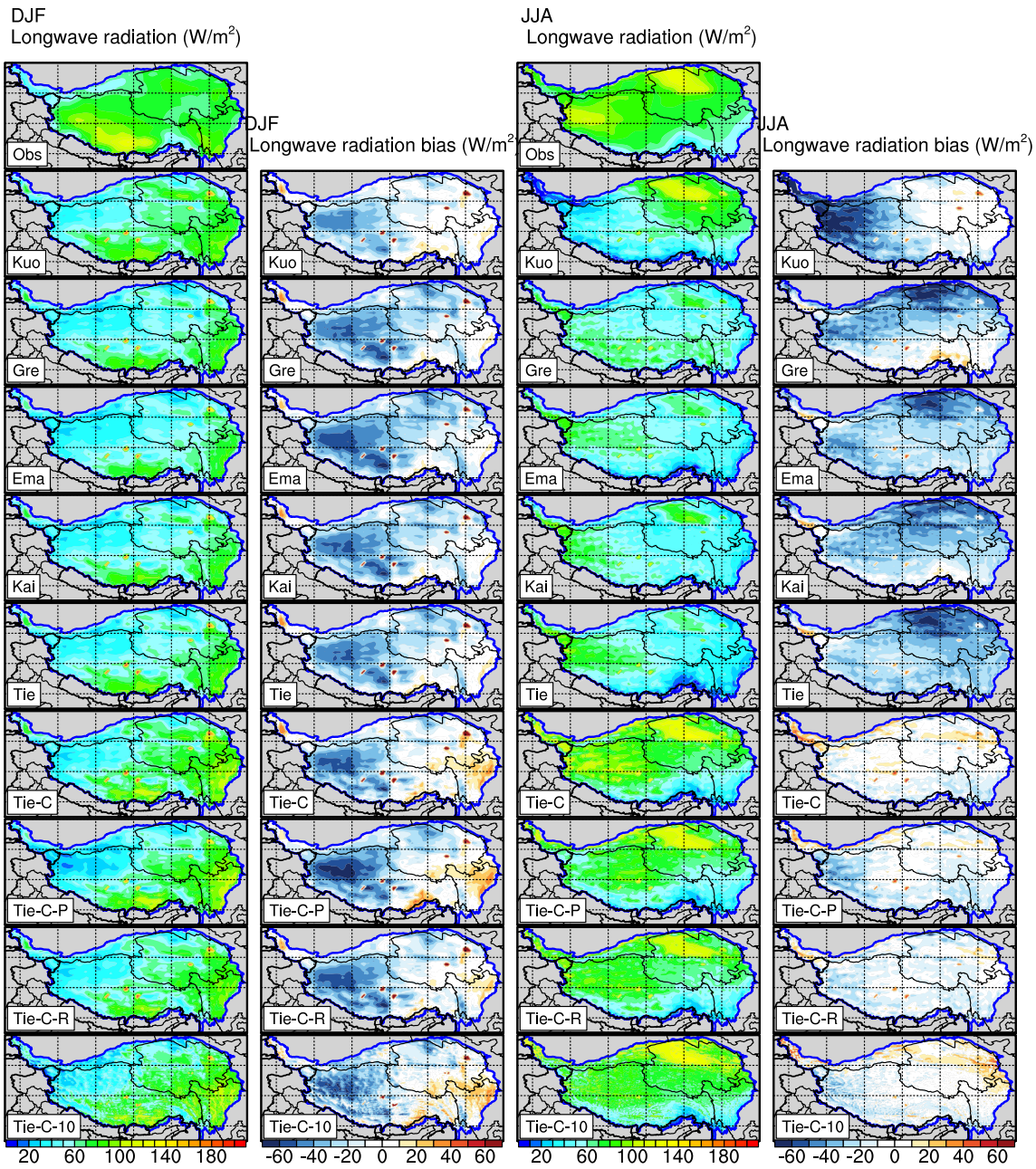

Fig. 5 Same as Fig. 3, but for surface net LW radiation

schemes show a stronger southerly flow in the south of the TP, which tends to transport more moisture to the TP and explains the precipitation overestimation. The wind bias in the southeast TP is reduced when using CLM as the land surface model, although the bias remains large in the westernmost TP. Despite this, all convective schemes, except the Kuo scheme, depict roughly similar biases over the TP. Due to the limited simulation domain, the wind field from the double-nested 10-km resolution simulation is not shown here because the large-scale circulation pattern could not be captured in this interior domain.

3.2 Basin scale evaluation

In this section, we concentrate on the simulation results for precipitation and the 2-m air temperature over the five major river basins in the TP that were previously discussed, creating the foundation for the investigation regarding coupling RegCM4 with a hydrological model in the near future.

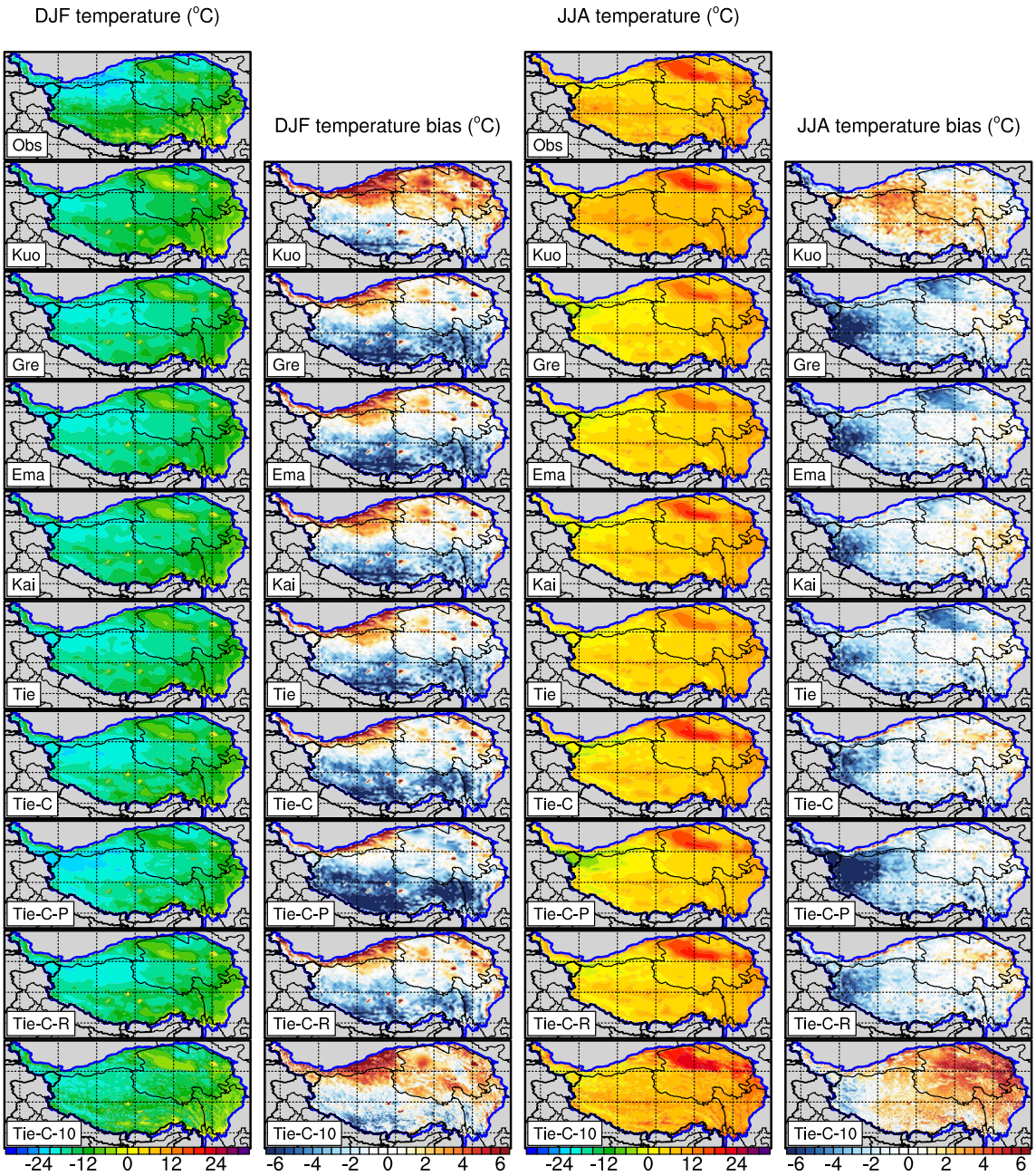

Fig. 6 Same as Fig. 3, but for 2-m air temperature

3.2.1 Seasonal cycles

Figure 8 shows the seasonal cycles of precipitation and the 2-m air temperature in the five river basins, upon which we decided to focus. For the entire TP, the ratio of the mean precipitation in the period of May–September to the annual precipitation exceeds 80% based on the observations. The Kuo scheme simulates an early peak in June; the Grell, Emanuel, and Kain model configurations simulate a late peak in August; while the Tiedtke configurations capture the observed peak in July very well. However, all the model configurations overestimate the observed precipitation, particularly the Emanuel scheme. The observations indicate a cold winter and warmer summer period with the highest temperatures occurring in July. The Kuo scheme is the only configuration that fails to capture the seasonal temperature pattern, simulating an early peak in June and overestimating the temperature in most months. The double-nested modelling at 10-km resolution tends to overestimate the temperature in summer,

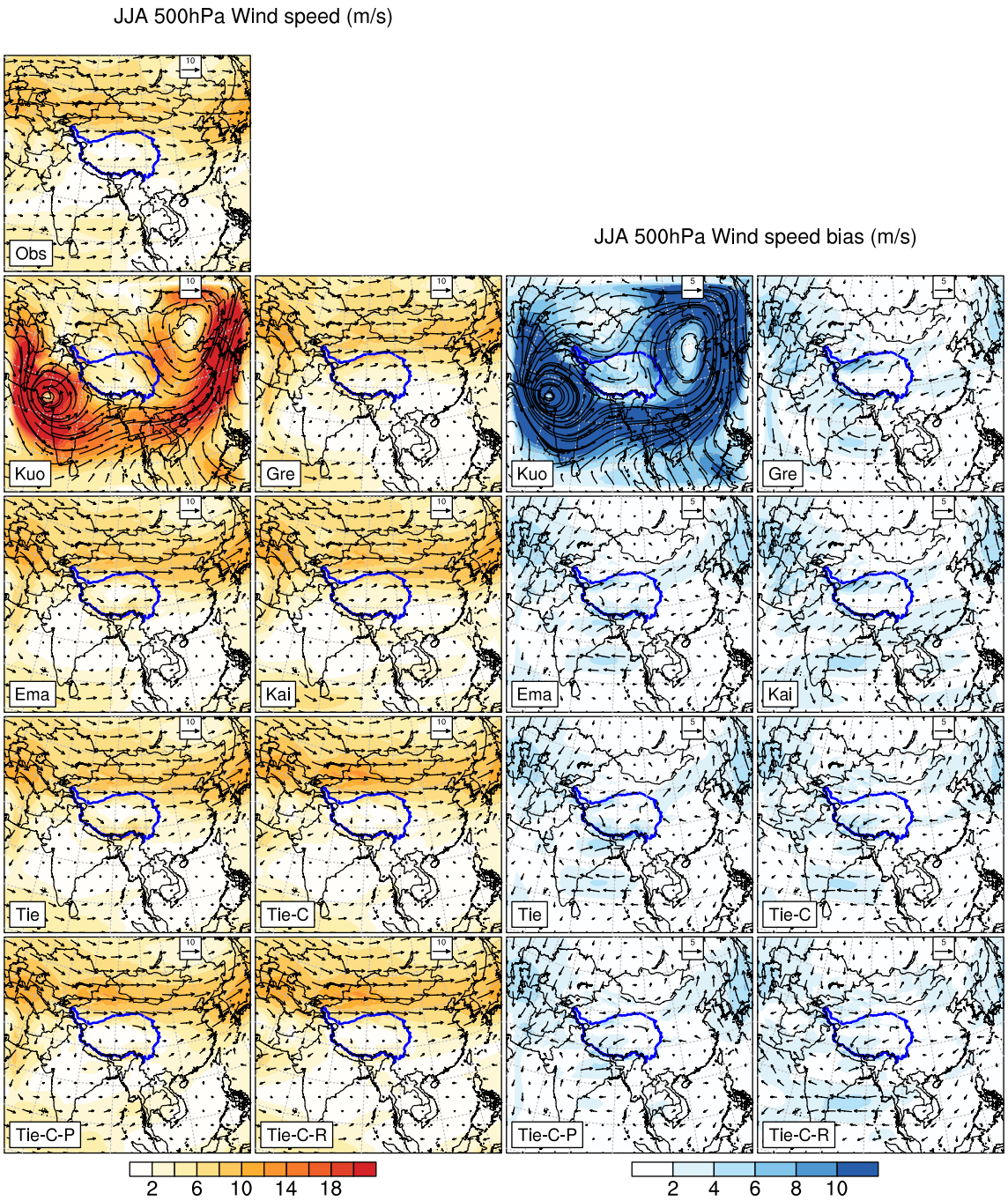

Fig. 7 Spatial distributions of JJA wind fields at 500 hPa (two leftmost panels) and associated wind field biases (two rightmost panels) derived from observations (first row) and simulations with different configurations. The colors indicate the wind speed, and the arrows indicate the direction and intensity

despite reproducing the seasonal cycle of the temperature well. All other model configurations reproduce the seasonal distribution of the temperature at 2 m well but tend to underestimate the temperature compared to the observations, particularly in the first half of the year. The simulation from Tiedtke combined with the CLM is closer to the observations compared to the other configurations.

Among the five basins, the source area of the Yellow River is located in the northeastern TP and contributes approximately 35% of the river's annual discharge (Lan et al. 2010; Yuan et al. 2015). Excluding that using the Kuo scheme, all model configurations capture the seasonal cycles of the precipitation and temperature well; however, the Emanuel, Tiedtke, and Grell schemes overestimate the observed

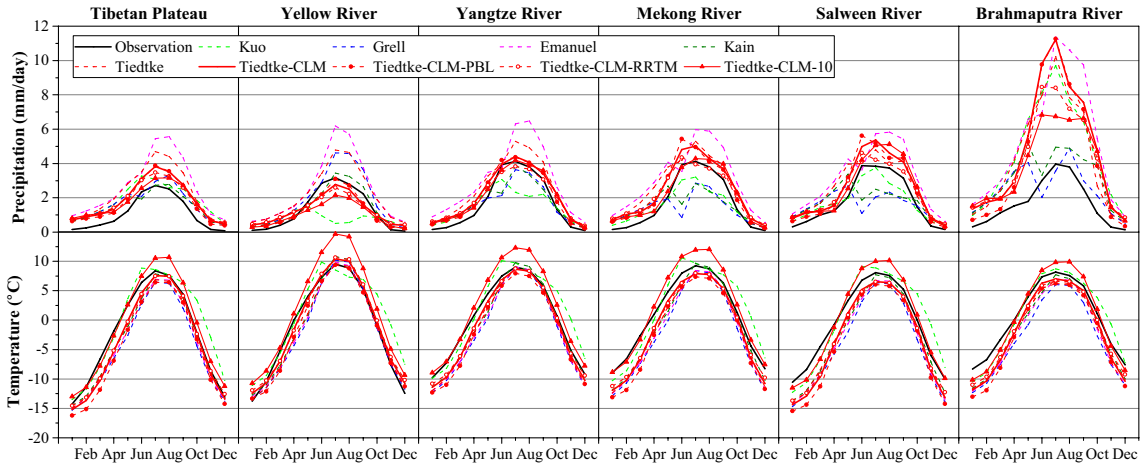

Fig. 8 Seasonal cycles of the yearly precipitation (top) and temperature (bottom) averaged over the whole TP and five subregions (left to right) for the given time period of 20 years (1989–2008)

precipitation, particularly in summer. The overestimation is reduced when the Tiedtke scheme is the coupled with the CLM land surface model.

The source region of the Yangtze River is located to the south of that of the Yellow River, and covers the largest area among the five river source regions. The seasonal cycles of precipitation and temperature are well captured by most model configurations. Tiedtke coupled with CLM continues to show the best performance among the configurations.

Meanwhile, the source regions of the Mekong River and Salween River are two south-north-oriented narrow basins located in the eastern TP, and cover the smallest area. Most of the model configurations are able to capture the seasonal cycles of temperature in these basins well, but have difficulty in reproducing the seasonal patterns of precipitation. For example, the Grell and Kain schemes simulate an unrealistically low precipitation in June and underestimate the observed summer precipitation. Furthermore, Emanuel consistently overestimates the precipitation in most months. Tiedtke also overestimates the precipitation and shows little improvement when coupled with CLM, although it captures the seasonal patterns of precipitation well.

The Brahmaputra River in the northern Himalayas has the highest elevation catchment of any of the world's great rivers, and the upper region is approximately 2000 km in length (You et al. 2007). All model configurations reproduced the seasonal temperature cycle with cold biases throughout the year, and in particular, they underestimate the temperature by more than 3 °C in the cold season (e.g., November–March). However, as shown in Fig. 8, all model configurations greatly overestimated the precipitation throughout the year, particularly the Kuo, Emanuel, and Tiedtke schemes, which overestimate the observed precipitation by more than 100%. A reduced overestimation was found to be characteristic of the Grell and Kain schemes, but they simulated unrealistically low precipitation in June. The CLM land surface model did not reduce the overestimation in the Brahmaputra River, but the model with the 10-km resolution did reduce the overestimation significantly compared with the 30-km resolution simulation (reduced from approximately 180% to 70%). This is primarily due to the relatively smooth topography in RegCM at the course resolution, which extends the rain-belt northward into the Plateau rather than limiting the rain-belt to the southern region of the Himalayas. A model with higher resolution could improve the precipitation simulation over this basin, although an overestimation might still occur.

In summary, the simulation from Tiedtke combined with the CLM model better reproduces the observed seasonal cycles of temperature and precipitation over the five subregions and the entire TP domain, compared with the other configurations investigated.

3.2.2 Interannual variability

The interannual variations of the yearly temperature and precipitation averaged over the whole TP and five subregions for the study period of 20 years (1989–2008) are shown in Fig. 9, including the results obtained for all the model configurations. Most of the experiments show a consistent wet and cold bias compared with the observation. The Emanuel scheme yields the largest wet bias in the whole TP domain. Meanwhile, the Grell scheme produces a relatively low bias for the precipitation but yields the largest cold bias for the temperature. Most models could simulate the interannual variations of the temperature well, with spatial correlation coefficients ranging from 0.54 to 0.85. However, the interannual variations of the precipitation were not captured by

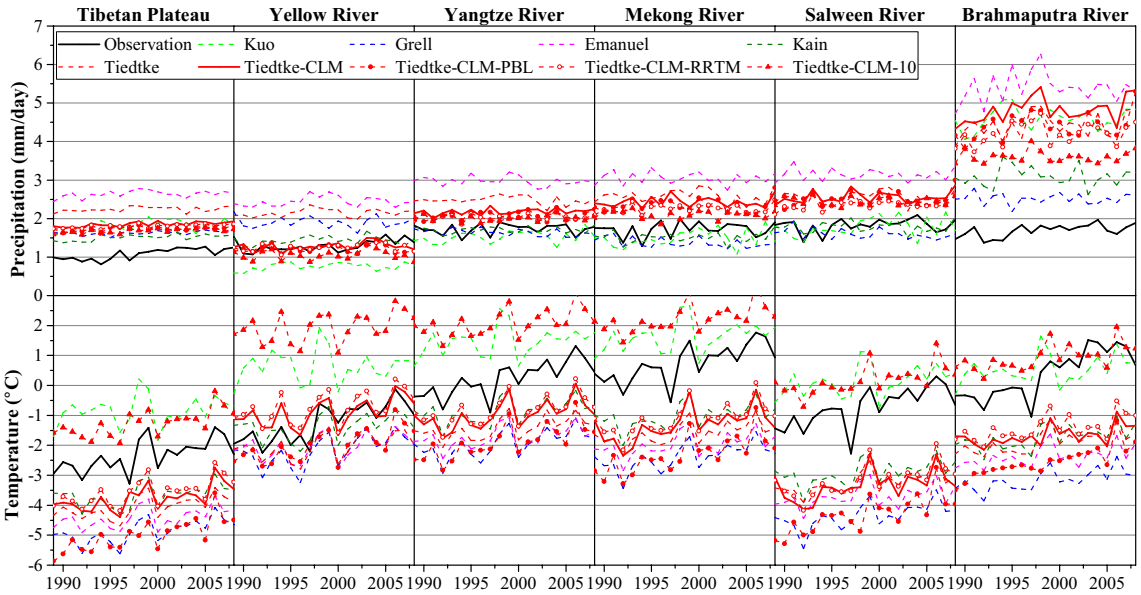

Fig. 9 Interannual variations of the yearly precipitation (top) and temperature (bottom) averaged over the whole TP and five subregions (left to right) for the given time period of 20 years (1989–2008)

most models, with an average correlation coefficient of 0.29. The Kuo scheme has the worst performance in reproducing the interannual variabilities of precipitation and temperature.

It is useful to evaluate the ability of the model to simulate the regional climatic trends. A good performance in this respect could reinforce the credibility of the model in future climate projections. The linear trend values of the observed and simulated precipitation and 2-m air temperature during the period 1989–2008 averaged over the entire TP and five subregions are shown in Fig. 10. The observed precipitation trend shows a predominantly positive value over the entire TP, particularly in the Yellow and Brahmaputra River basins, where an increase of more than 10%/decade was found. This trend signal has been captured by most models, although they underestimate the magnitude. For the Yangtze, Mekong, and Salween River basins, where the observed precipitation trends are not significant, little agreement was found between the different simulations. The observed 2-m

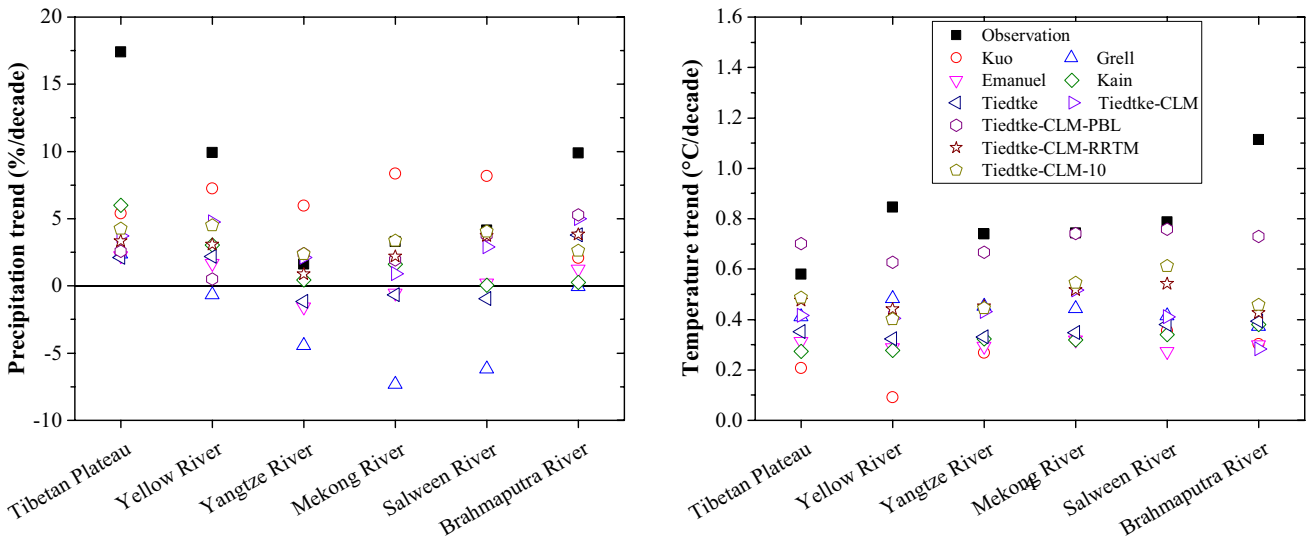

Fig. 10 Observed and simulated annual precipitation and temperature trends during the period 1989–2008 averaged over the whole TP and five subregions

air temperature shows a pronounced warming during this period. Most models can reproduce this positive trend over the whole domain, though they also underestimate the magnitude. This underestimation of the warming trend is partly due to the fact that the ERA-interim reanalysis forcing data also underestimates the warming trend over the TP (Gao et al. 2015). The results indicate that there are numerous qualitative agreements between the observations and model simulations, and the simulated trend was influenced by the model configurations. It should be noted that the warming and wetting trends in the 20-year study period are more significant than those in the last 50 years (Xu et al. 2008). In addition, due to the large magnitude of interannual variability and the existence of multi-decadal variability (Ziegler et al. 2005), the study period is too short for a meaningful climate trend analysis, particularly for precipitation.

3.2.3 Precipitation intensities

Figure 11 displays the percentage distribution of the daily precipitation frequency and amount during the period from 1989 to 2008, averaged over the entire domain of the TP and five subregions for all experiments. Generally, the frequency and amount of daily precipitation events within the given intervals of intensity were well simulated by most experiments. However, the dry days (e.g., <0.1 mm/day) were underestimated compared with the observations in most configurations. The results for the dry days show less underestimation in the five subregions compared with the entire TP, which indicates a more significant underestimation in the dry western TP. This is partly because RegCM usually "drizzles" excessively at the lowest intensities, particularly over the dry region (Halenka et al. 2006; Seth et al. 2004).

It is evident that the maximum frequency of the observed precipitation (0.1–1 mm/day) was well captured in most configurations. However, the model tends to overestimate the frequency of light (1.0–5.0 mm/day), and particularly moderate (5.0–10.0 mm/day) and heavy (>10 mm/day) precipitation. It also overestimates the amount of heavy precipitation compared to the observed data, particularly in the Brahmaputra River basin. The model underestimated the amount of light precipitation and overestimated the amount of precipitation with an intensity higher than 7 mm/day in the Brahmaputra River basin, indicating that, in general, the overestimation of the precipitation in this basin derives from high-intensity events, which mainly occur in summer. This overestimation is mostly related to the enhancement of the summer convective precipitation because of the relatively coarse horizontal resolution of the exceptionally complex terrain along the Himalayas in this area. In fact, we found that the configurations (for example, the Emanuel cumulous convection scheme) with a wet bias in the annual precipitation are associated with an overestimation of the precipitation amounts for events with precipitation at rates higher than 10 mm/day. This is consistent with the results from Zhang et al. who argued that convective activity is overestimated in the Emanuel scheme, generating excessively heavy precipitation (Zhang et al. 2015). These results indicate that it remains difficult for the current version of RegCM4 to simulate extreme precipitation events in the TP.

4 Summary and conclusions

This paper presented a comprehensive evaluation of RegCM4 over the TP. Our analyses focus on climate factors including the precipitation, cloud cover, surface net radiation, 2-m air temperature, and surface wind circulation. We compared the performance of the model with nine distinct physics configurations, which differ in the parameterizations of cumulus parameterization, land surface processes, PBL, and radiation schemes. Furthermore, five major river basins were selected to thoroughly investigate the performance of RegCM4 on the basin scale.

The results indicate that the modeled climate is highly sensitive to the parametrizations selected for the representation of the sub-grid scale processes. In particular, precipitation is sensitive to the cumulus parameterization, with the Emanuel and Tiedtke schemes exhibiting a better performance in reproducing the spatial distribution of 20 years of mean precipitation, though they significantly overestimate the rainfall compared with the other schemes. However, the overestimation of precipitation is reduced when the model employs the CLM land surface model instead of the default BATS model. In addition, the model characterized by a higher resolution (10 km) shows better performance in reproducing the magnitude and distribution of the mean precipitation.

Compared with the convection schemes, a change of land surface model results in larger changes in cloud cover and surface radiation. Generally, the CLM results in the prediction of less mean cloud cover and more surface shortwave radiation and surface longwave radiation over the TP compared with the BATS scheme. In contrast, the UW PBL parameterization and RRTM radiation scheme tend to result in increased cloud cover and less surface shortwave and longwave radiations compared with the default options for these processes.

Most model configurations were able to reproduce the spatial distribution of 2-m air temperature well over the TP. However, significant cold biases were found to exist in both winter and summer, particularly in the western and southern TP. These cold biases may be partly caused by the systematic biases in the ERA forcing data and the overestimation in the observations associated with the fact that most meteorological stations lie in valleys (Wang et al. 2016a, b). Analogously,

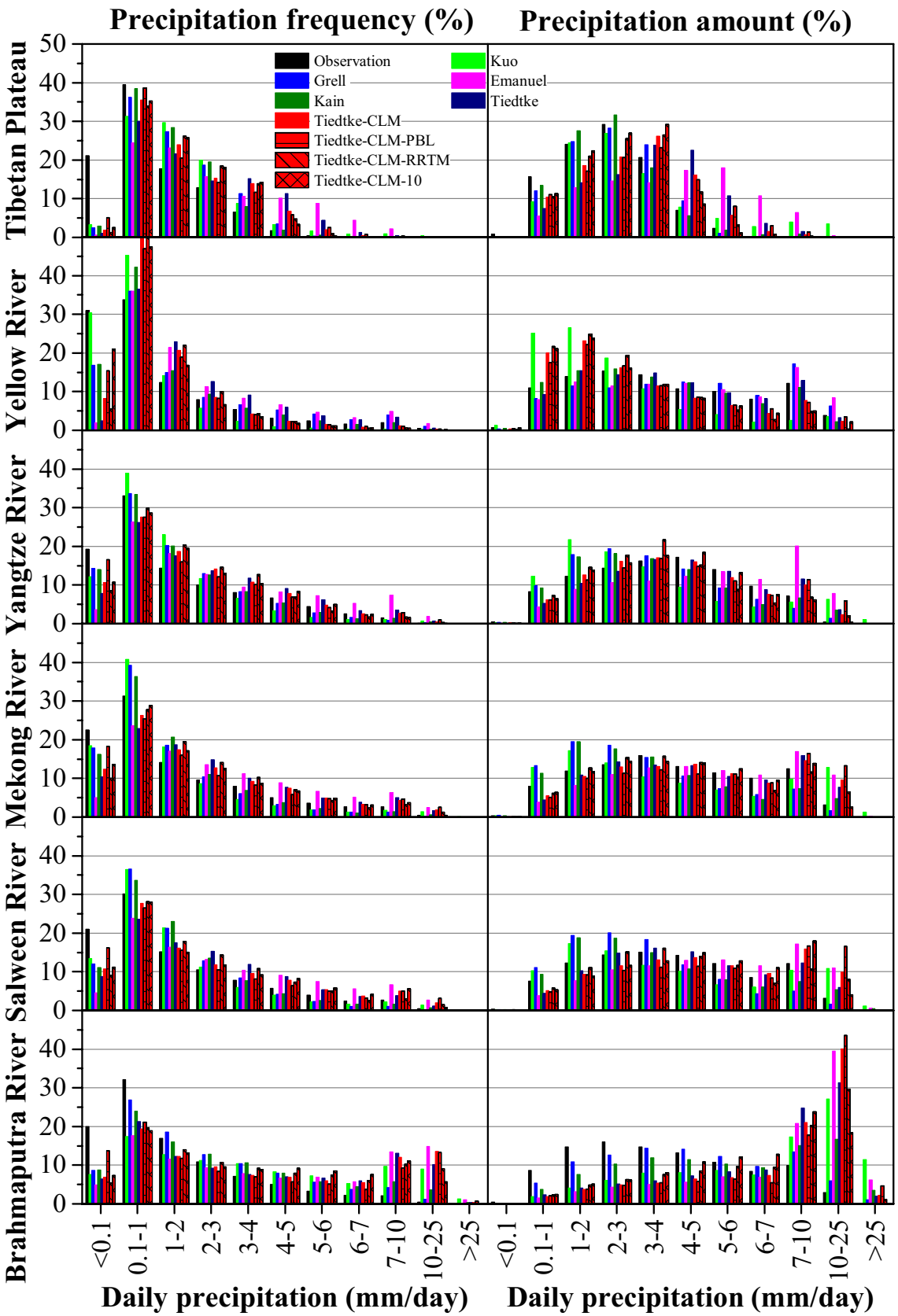

Fig. 11 Ratio distribution of averaged observation and simulated daily precipitation frequency (left panel) and amount (right panel) over the whole TP and five subregions (from top to bottom) during 1989–2008

uncertainties in the observation dataset over the TP may also contribute to the model wet bias. Ma et al. (2015) concluded that an overall mean of 27% negative bias was found in the collected precipitation data from 241 meteorological stations across the TP and surrounding regions from ten countries; in particular, the largest bias was found in the unshielded Chinese standard precipitation gauge, which was used in the central TP region.

At the basin scale, most models were able to simulate the seasonal cycle and interannual variations of temperature well over the five different basins. However, the seasonal distribution and interannual variations of precipitation were not captured by most models. The simulated precipitation and temperature by the Tiedtke scheme combined with the CLM is closest to the observations among the simulations produced using nine different model configurations. The increasing trends for the historical precipitation and temperature was captured by most models, though they underestimate the magnitude. The most significant overestimation of precipitation was found in the Brahmaputra River basin, and this overestimation derives from high-intensity events.

Based on the above results, it can be concluded that the model is highly sensitive to the choice of configuration over the TP. Overall, the Tiedtke scheme combined with the CLM land surface model yields better results for seasonal mean climate and basin scale climate simulations compared to other model configurations. Previous studies have recommended the Grell and Emanuel schemes for South Asia and East Asia (Li et al. 2016; Maity et al. 2017; Raju et al. 2015; Zhang et al. 2015). However, over most parts of the TP and the five major source basins, our results suggest the Tiedtke scheme is superior, especially when it is combined with the CLM. In the near future, we will continue to perform long-period climate simulations to generate an ensemble of future climate projections and use them to investigate the response of terrestrial hydrological processes over the TP to climate change.

Acknowledgements This work was supported by the National Key R&D Program of China (No. 2016YFC0402706, 2016YFC0402710), the National Natural Science Foundation of China (No. 51539003, 41761134090, 41807149, 51709074), the Fundamental Research Funds for the Central Universities (2019B10614). The research of WRP at the University of Toronto is supported by NSERC Discovery Grant A 9627. The observation dataset used in this study was developed by Data Assimilation and Modeling Center for Tibetan Multi-spheres, Institute of Tibetan Plateau Research, Chinese Academy of Sciences. The simulations discussed in this paper were performed in part on the SciNet High Performance Computing facility of the University of Toronto which is a component of the Compute Canada HPC platform.

References

Ali S, Dan L, Fu C, Yang Y (2015) Performance of convective parameterization schemes in Asia using RegCM: simulations in three typical regions for the period 1998–2002. Adv Atmos Sci 32:715–730. https://doi.org/10.1007/s00376-014-4158-4

Almazroui M (2015) RegCM4 in climate simulation over CORDEX-MENA/Arab domain: selection of suitable domain, convection and land-surface schemes. Int J Climatol 36:236–251. https://doi.org/10.1002/joc.4340

Anthes RA (1977) A cumulus parameterization scheme utilizing a one-dimensional cloud model. Mon Weather Rev 105:270–286. https://doi.org/10.1175/1520-0493(1977)105%3c0270:ACPSUA%3e2.0.CO;2

Bao X, Zhang F (2012) Evaluation of NCEP–CFSR, NCEP–NCAR, ERA-Interim, and ERA-40 Reanalysis Datasets against Independent Sounding Observations over the Tibetan Plateau. J Clim 26:206–214. https://doi.org/10.1175/JCLI-D-12-00056.1

Bretherton CS, McCaa JR, Grenier H (2004) A new parameterization for shallow cumulus convection and its application to marine subtropical cloud-topped boundary layers. Part I: description and 1D results. Mon Weather Rev 132:864–882. https://doi.org/10.1175/1520-0493(2004)132%3c0864:ANPFSC%3e2.0.CO;2

Chen F, Avissar R (1994) Impact of land-surface moisture variability on local shallow convective cumulus and precipitation in large-scale models. J Appl Meteorol 33:1382–1401. https://doi.org/10.1175/1520-0450(1994)033%3c1382:IOLSMV%3e2.0.CO;2

Chen X, Škerlak B, Rotach MW, Añel JA, Su Z, Ma Y, Li M (2016) Reasons for the extremely high-ranging planetary boundary layer over the western Tibetan Plateau in winter. J Atmos Sci 73:2021–2038. https://doi.org/10.1175/JAS-D-15-0148.1

Cui X, Graf H (2009) Recent land cover changes on the Tibetan Plateau: a review. Clim Change 94:47–61. https://doi.org/10.1007/s10584-009-9556-8

Dash SK, Pattnayak KC, Panda SK, Vaddi D, Mamgain A (2014) Impact of domain size on the simulation of Indian summer monsoon in RegCM4 using mixed convection scheme and driven by HadGEM2. Clim Dyn. https://doi.org/10.1007/s00382-014-2420-1

Dickinson RE, Henderson-Sellers A, Kennedy PJ (1993) Biosphere-atmosphere transfer scheme (BATS) version 1 as coupled to the NCAR community climate model. National Center for Atmospheric Research

Dimri AP, Niyogi D (2013) Regional climate model application at subgrid scale on Indian winter monsoon over the western Himalayas. Int J Climatol 33:2185–2205. https://doi.org/10.1002/joc.3584

D'Orgeville M, Peltier WR, Erler AR, Gula J (2014) Climate change impacts on Great Lakes Basin precipitation extremes. J Geophys Res Atmos 119(10):710–799, 812. https://doi.org/10.1002/2014jd021855

Emanuel KA (1991) A scheme for representing cumulus convection in large-scale models. J Atmos Sci 48:2313–2329. https://doi.org/10.1175/1520-0469(1991)048%3c2313:ASFRCC%3e2.0.CO;2

Erler AR, Peltier WR (2017) Projected hydroclimatic changes in two major river basins at the Canadian west coast based on high-resolution regional climate simulations. J Clim 30:8081–8105. https://doi.org/10.1175/JCLI-D-16-0870.1

Gao X, Xu Y, Zhao Z, Pal JS, Giorgi F (2006) On the role of resolution and topography in the simulation of East Asia precipitation. Theor Appl Climatol 86:173–185. https://doi.org/10.1007/s00704-005-0214-4

Gao X, Shi Y, Giorgi F (2011) A high resolution simulation of climate change over China. Sci China Earth Sci 54:462–472. https://doi.org/10.1007/s11430-010-4035-7

Gao X, Shi Y, Zhang D, Giorgi F (2012) Climate change in China in the 21st century as simulated by a high resolution regional climate

model. Chin Sci Bull 57:1188–1195. https://doi.org/10.1007/s11434-011-4935-8
Gao Y, Xu J, Chen D (2015) Evaluation of WRF mesoscale climate simulations over the Tibetan Plateau during 1979–2011. J Clim 28:2823–2841. https://doi.org/10.1175/JCLI-D-14-00300.1
Gao X, Shi Y, Giorgi F (2016) Comparison of convective parameterizations in RegCM4 experiments over China with CLM as the land surface model. Atmos Ocean Sci Lett 9:246–254. https://doi.org/10.1080/16742834.2016.1172938
Gao Y, Xiao L, Chen D, Chen F, Xu J, Xu Y (2017) Quantification of the relative role of land-surface processes and large-scale forcing in dynamic downscaling over the Tibetan Plateau. Clim Dyn 48:1705–1721. https://doi.org/10.1007/s00382-016-3168-6
García-Díez M, Fernández J, Vautard R (2015) An RCM multi-physics ensemble over Europe: multi-variable evaluation to avoid error compensation. Clim Dyn 45:3141–3156. https://doi.org/10.1007/s00382-015-2529-x
Giorgi F et al (2012) RegCM4: model description and preliminary tests over multiple CORDEX domains. Clim Res 52:7–29. https://doi.org/10.3354/cr01018
Grell GA (1993) Prognostic evaluation of assumptions used by cumulus parameterizations. Mon Weather Rev 121:764–787. https://doi.org/10.1175/1520-0493(1993)121%3c0764:PEOAUB%3e2.0.CO;2
Grenier H, Bretherton CS (2001) A moist PBL parameterization for large-scale models and its application to subtropical cloud-topped marine boundary layers. Mon Weather Rev 129:357–377. https://doi.org/10.1175/1520-0493(2001)129%3c0357:AMPPFL%3e2.0.CO;2
Gu H, Wang G, Yu Z, Mei R (2012) Assessing future climate changes and extreme indicators in east and south Asia using the RegCM4 regional climate model. Clim Change 114:301–317. https://doi.org/10.1007/s10584-012-0411-y
Gu H et al (2015) Assessing CMIP5 general circulation model simulations of precipitation and temperature over China. Int J Climatol 35:2431–2440. https://doi.org/10.1002/joc.4152
Gu H, Yu Z, Yang C, Ju Q, Yang T, Zhang D (2018) High-resolution ensemble projections and uncertainty assessment of regional climate change over China in CORDEX East Asia. Hydrol Earth Syst Sci 22:3087–3103. https://doi.org/10.5194/hess-22-3087-2018
Gula J, Peltier WR (2012) Dynamical downscaling over the Great Lakes Basin of North America using the WRF regional climate model: the impact of the Great Lakes System on regional greenhouse warming. J Clim 25:7723–7742. https://doi.org/10.1175/JCLI-D-11-00388.1
Guo D, Wang H (2012) The significant climate warming in the northern Tibetan Plateau and its possible causes. Int J Climatol 32:1775–1781. https://doi.org/10.1002/joc.2388
Guo D, Sun J, Yu E (2018) Evaluation of CORDEX regional climate models in simulating temperature and precipitation over the Tibetan Plateau. Atmos Ocean Sci Lett 11:219–227. https://doi.org/10.1080/16742834.2018.1451725
Guo D, Sun J, Yang K, Pepin N, Xu Y, Xu Z, Wang H (2019) Satellite data reveal southwestern Tibetan Plateau cooling since 2001 due to snow-albedo feedback. Int J Climatol. https://doi.org/10.1002/joc.6292
Halenka T, Kalvová J, Chládová Z, Demeterová A, Zemánková K, Belda M (2006) On the capability of RegCM to capture extremes in long term regional climate simulation—comparison with the observations for Czech Republic. Theor Appl Climatol 86:125–145. https://doi.org/10.1007/s00704-005-0205-5
He J, Yang K, Tang W, Lu H, Qin J, Chen Y, Li X (2020) The first high-resolution meteorological forcing dataset for land process studies over China. Sci Data 7:25. https://doi.org/10.1038/s41597-020-0369-y
Holtslag AAM, Boville BA (1993) Local versus nonlocal boundary-layer diffusion in a global climate model. J Clim 6:1825–1842. https://doi.org/10.1175/1520-0442(1993)006%3c1825:LVNBLD%3e2.0.CO;2
Huang W, Chan JCL, Au-Yeung AYM (2013) Regional climate simulations of summer diurnal rainfall variations over East Asia and Southeast China. Clim Dyn 40:1625–1642. https://doi.org/10.1007/s00382-012-1457-2
Huo Y, Peltier WR (2019) Dynamically downscaled climate simulations of the Indian monsoon in the instrumental era: physics parameterization impacts and precipitation extremes. J Appl Meteorol Climatol 58:831–852. https://doi.org/10.1175/JAMC-D-18-0226.1
Im E, Ahn J, Remedio AR, Kwon W (2008) Sensitivity of the regional climate of East/Southeast Asia to convective parameterizations in the RegCM3 modelling system. Part 1: focus on the Korean peninsula. Int J Climatol 28:1861–1877. https://doi.org/10.1002/joc.1664
Immerzeel WW, van Beek LPH, Bierkens MFP (2010) Climate change will affect the Asian water towers. Science 328:1382–1385. https://doi.org/10.1126/science.1183188
IPCC (2013) Climate change 2013: the physical basis. Contribution of Working Group 1 to the Fifth Assessment Report of the IPCC. Cambridge University Press, New York
Ji Z, Kang S (2013) Double-nested dynamical downscaling experiments over the Tibetan Plateau and their projection of climate change under two RCP scenarios. J Atmos Sci 70:1278–1290. https://doi.org/10.1175/JAS-D-12-0155.1
Jiang D, Tian Z, Lang X (2016) Reliability of climate models for China through the IPCC Third to Fifth Assessment Reports. Int J Climatol 36:1114–1133. https://doi.org/10.1002/joc.4406
Jiang X, Wu Y, Li Y, Shu J (2019) Simulation of interannual variability of summer rainfall over the Tibetan Plateau by the Weather Research and Forecasting model. Int J Climatol 39:756–767. https://doi.org/10.1002/joc.5840
Kain JS, Fritsch JM (1993) Convective parameterization for mesoscale models: the Kain–Fritsch scheme. In: Emanuel KA, Raymond DJ (eds) The representation of cumulus convection in numerical models. American Meteorological Society, Boston, pp 165–170. https://doi.org/10.1007/978-1-935704-13-3_16
Kang S, Im E, Ahn J (2014) The impact of two land-surface schemes on the characteristics of summer precipitation over East Asia from the RegCM4 simulations. Int J Climatol 34:3986–3997. https://doi.org/10.1002/joc.3998
Kiehl JT, Hack JJ, Bonan GB, Boville BA, Breigleb BP, Williamson D, Rasch P (1996) Description of the NCAR community climate model (CCM3). National Center for Atmospheric Research
Kim J, Jung H, Mechoso CR, Kang H (2008) Validation of a multidecadal RCM hindcast over East Asia. Glob Planet Change 61:225–241. https://doi.org/10.1016/j.gloplacha.2006.05.006
Koné B et al (2018) Sensitivity study of the regional climate model RegCM4 to different convective schemes over West Africa. Earth Syst Dyn 9:1261–1278. https://doi.org/10.5194/esd-9-1261-2018
Lan Y, Zhao G, Zhang Y, Wen J, Liu J, Hu X (2010) Response of runoff in the source region of the Yellow River to climate warming. Quatern Int 226:60–65. https://doi.org/10.1016/j.quaint.2010.03.006
Lange S, Rockel B, Volkholz J, Bookhagen B (2015) Regional climate model sensitivities to parametrizations of convection and non-precipitating subgrid-scale clouds over South America. Clim Dyn 44:2839–2857. https://doi.org/10.1007/s00382-014-2199-0
Li W, Feng J, Chen S, Wang L (2012) Relationship between wintertime precipitation in South China and air–sea heat fluxes. Atmos Sci Lett 13:113–119. https://doi.org/10.1002/asl.370
Li BQ, Yu ZB, Liang ZM, Acharya K (2014) Hydrologic response of a high altitude glacierized basin in the central Tibetan Plateau.

Glob Planet Change 118:69–84. https://doi.org/10.1016/j.gloplacha.2014.04.006
Li Y, Tam C, Huang W, Cheung KKW, Gao Z (2016) Evaluating the impacts of cumulus, land surface and ocean surface schemes on summertime rainfall simulations over East-to-southeast Asia and the western north Pacific by RegCM4. Clim Dyn 46:2487–2505. https://doi.org/10.1007/s00382-015-2714-y
Li BQ, Zhang JY, Yu ZB, Liang ZM, Chen L, Acharya K (2017) Climate change driven water budget dynamics of a Tibetan inland lake. Glob Planet Change 150:70–80. https://doi.org/10.1016/j.gloplacha.2017.02.003
Lin C, Chen D, Yang K, Ou T (2018) Impact of model resolution on simulating the water vapor transport through the central Himalayas: implication for models' wet bias over the Tibetan Plateau. Clim Dyn 51:3195–3207. https://doi.org/10.1007/s00382-018-4074-x
Liu X, Chen B (2000) Climatic warming in the Tibetan Plateau during recent decades. Int J Climatol 20:1729–1742. https://doi.org/10.1002/1097-0088(20001130)20:14%3c1729:AID-JOC556%3e3.0.CO;2-Y
Liu H, Zhang D, Wang B (2010) Impact of horizontal resolution on the regional climate simulations of the summer 1998 extreme rainfall along the Yangtze River Basin. J Geophys Res Atmos 115:D12115. https://doi.org/10.1029/2009JD012746
Liu M, Tang R, Li Z, Yan G (2019) Integration of two semi-physical models of terrestrial evapotranspiration using the China Meteorological Forcing Dataset. Int J Remote Sens 40:1966–1980. https://doi.org/10.1080/01431161.2018.1482026
Ma Y, Zhang Y, Yang D, Farhan SB (2015) Precipitation bias variability versus various gauges under different climatic conditions over the Third Pole Environment (TPE) region. Int J Climatol 35:1201–1211. https://doi.org/10.1002/joc.4045
Maity S, Satyanarayana ANV, Mandal M, Nayak S (2017) Performance evaluation of land surface models and cumulus convection schemes in the simulation of Indian summer monsoon using a regional climate model. Atmos Res 197:21–41. https://doi.org/10.1016/j.atmosres.2017.06.023
Maussion F, Scherer D, Finkelnburg R, Richters J, Yang W, Yao T (2011) WRF simulation of a precipitation event over the Tibetan Plateau, China—an assessment using remote sensing and ground observations. Hydrol Earth Syst Sci 15:1795–1817. https://doi.org/10.5194/hess-15-1795-2011
Maussion F, Scherer D, Mölg T, Collier E, Curio J, Finkelnburg R (2014) Precipitation seasonality and variability over the Tibetan Plateau as resolved by the high Asia reanalysis. J Clim 27:1910–1927. https://doi.org/10.1175/JCLI-D-13-00282.1
Ménégoz M, Gallée H, Jacobi HW (2013) Precipitation and snow cover in the Himalaya: from reanalysis to regional climate simulations. Hydrol Earth Syst Sci 17:3921–3936. https://doi.org/10.5194/hess-17-3921-2013
Mlawer EJ, Taubman SJ, Brown PD, Iacono MJ, Clough SA (1997) Radiative transfer for inhomogeneous atmospheres: RRTM, a validated correlated-k model for the longwave. J Geophys Res Atmos 102:16663–16682. https://doi.org/10.1029/97JD00237
Nan S, Zhao P, Yang S, Chen J (2009) Springtime tropospheric temperature over the Tibetan Plateau and evolutions of the tropical Pacific SST. J Geophys Res Atmos. https://doi.org/10.1029/2008JD011559
Oh S, Park J, Lee S, Suh M (2014) Assessment of the RegCM4 over East Asia and future precipitation change adapted to the RCP scenarios. J Geophys Res Atmos 119:2913–2927. https://doi.org/10.1002/2013JD020693
Oleson KW et al (2008) Improvements to the Community Land Model and their impact on the hydrological cycle. J Geophys Res Biogeosci 113:G1021. https://doi.org/10.1029/2007JG000563
Pal JS et al (2007) The ICTP RegCM3 and RegCNET: regional climate modeling for the developing world. Bull Am Math Soc 88:1395–1409. https://doi.org/10.1175/BAMS-88-9-1395
Park J, Oh S, Suh M (2013) Impacts of boundary conditions on the precipitation simulation of RegCM4 in the CORDEX East Asia domain. J Geophys Res Atmos 118:1652–1667. https://doi.org/10.1002/jgrd.50159
Peltier WR, D'Orgeville M, Erler AR, Xie FY (2018) Uncertainty in future summer precipitation in the Laurentian Great Lakes basin: dynamical downscaling and the influence of continental-scale processes on regional climate change. J Clim 31:2651–2673. https://doi.org/10.1175/JCLI-D-17-0416.1
Pessacg NL et al (2014) The surface radiation budget over South America in a set of regional climate models from the CLARIS-LPB project. Clim Dyn 43:1221–1239. https://doi.org/10.1007/s00382-013-1916-4
Qin J, Yang K, Liang S, Guo X (2009) The altitudinal dependence of recent rapid warming over the Tibetan Plateau. Clim Change 97:321–327. https://doi.org/10.1007/s10584-009-9733-9
Qiu J (2008) China: the third pole. Nature 454:393–396. https://doi.org/10.1038/454393a
Raju PVS, Bhatla R, Almazroui M, Assiri M (2015) Performance of convection schemes on the simulation of summer monsoon features over the South Asia CORDEX domain using RegCM-4.3. Int J Climatol 35:4695–4706. https://doi.org/10.1002/joc.4317
Rangwala I, Miller JR (2012) Climate change in mountains: a review of elevation-dependent warming and its possible causes. Clim Change 114:527–547. https://doi.org/10.1007/s10584-012-0419-3
Rauscher SA, Seth A, Qian JH, Camargo SJ (2006) Domain choice in an experimental nested modeling prediction system for South America. Theor Appl Climatol 86:229–246. https://doi.org/10.1007/s00704-006-0206-z
Rossow WB, Schiffer RA (1999) Advances in understanding clouds from ISCCP. Bull Am Meteorol Soc 80:2261–2288. https://doi.org/10.1175/1520-0477(1999)080%3c2261:AIUCFI%3e2.0.CO;2
Samouly AA, Luong CN, Li Z, Smith S, Baetz B, Ghaith M (2018) Performance of multi-model ensembles for the simulation of temperature variability over Ontario, Canada. Environ Earth Sci 77:524. https://doi.org/10.1007/s12665-018-7701-2
Seth A, Rojas M, Liebmann B, Qian JH (2004) Daily rainfall analysis for South America from a regional climate model and station observations. Geophys Res Lett 31:L7213. https://doi.org/10.1029/2003GL019220
Seth A, Rauscher SA, Camargo SJ, Qian JH, Pal JS (2007) RegCM3 regional climatologies for South America using reanalysis and ECHAM global model driving fields. Clim Dyn 28:461–480. https://doi.org/10.1007/s00382-006-0191-z
Shi Y, Gao X, Zhang D, Giorgi F (2011) Climate change over the Yarlung Zangbo-Brahmaputra River Basin in the 21st century as simulated by a high resolution regional climate model. Quatern Int 244:159–168. https://doi.org/10.1016/j.quaint.2011.01.041
Shi Y, Wang G, Gao X (2018) Role of resolution in regional climate change projections over China. Clim Dyn 51:2375–2396. https://doi.org/10.1007/s00382-017-4018-x
Sinha P, Mohanty UC, Kar SC, Kumari S (2014) Role of the Himalayan orography in simulation of the Indian summer monsoon using RegCM3. Pure Appl Geophys 171:1385–1407. https://doi.org/10.1007/s00024-013-0675-9
Song F, Zhou T (2013) Interannual variability of east asian summer monsoon simulated by CMIP3 and CMIP5 AGCMs: skill dependence on Indian Ocean-Western Pacific anticyclone teleconnection. J Clim 27:1679–1697. https://doi.org/10.1175/JCLI-D-13-00248.1

Song J, Kang H, Byun Y, Hong S (2010) Effects of the Tibetan Plateau on the Asian summer monsoon: a numerical case study using a regional climate model. Int J Climatol 30:743–759. https://doi.org/10.1002/joc.1906

Sperber KR et al (2013) The Asian summer monsoon: an intercomparison of CMIP5 vs. CMIP3 simulations of the late 20th century. Clim Dyn 41:2711–2744. https://doi.org/10.1007/s00382-012-1607-6

Stackhouse JP, Gupta S, Cox S, Mikovitz C, Zhang T, Hinkelman L (2011) The NASA/GEWEX surface radiation budget release 3.0: 24.5-year dataset. GEWEX News 21:10–12

Steiner AL et al (2009) Land surface coupling in regional climate simulations of the West African monsoon. Clim Dyn 33:869–892. https://doi.org/10.1007/s00382-009-0543-6

Su F, Duan X, Chen D, Hao Z, Cuo L (2013) Evaluation of the global climate models in the CMIP5 over the Tibetan Plateau. J Clim 26:3187–3208. https://doi.org/10.1175/JCLI-D-12-00321.1

Sun H, Liu X, Pan Z (2017) Direct radiative effects of dust aerosols emitted from the Tibetan Plateau on the East Asian summer monsoon—a regional climate model simulation. Atmos Chem Phys 17:13731–13745. https://doi.org/10.5194/acp-17-13731-2017

Tapiador FJ, Navarro A, Moreno R, Sánchez JL, García-Ortega E (2020) Regional climate models: 30 years of dynamical downscaling. Atmos Res 235:104785. https://doi.org/10.1016/j.atmosres.2019.104785

Tiedtke M (1989) A comprehensive mass flux scheme for cumulus parameterization in large-scale models. Mon Weather Rev 117:1779–1800. https://doi.org/10.1175/1520-0493(1989)117%3c1779:ACMFSF%3e2.0.CO;2

Wang A, Zeng X (2012) Evaluation of multireanalysis products with in situ observations over the Tibetan Plateau. J Geophys Res Atmos 117:D5102. https://doi.org/10.1029/2011JD016553

Wang B, Bao Q, Hoskins B, Wu G, Liu Y (2008) Tibetan Plateau warming and precipitation changes in East Asia. Geophys Res Lett 35:L14702. https://doi.org/10.1029/2008GL034330

Wang X, Yang M, Wan G, Chen X, Pang G (2013) Qinghai-Xizang (Tibetan) Plateau climate simulation using the regional climate model RegCM3. Clim Res 57:173–186. https://doi.org/10.3354/cr01167

Wang X, Yang M, Pang G (2014) Sensitivity of regional climate simulations to land-surface schemes on the Tibetan Plateau. Clim Res 62:25–43. https://doi.org/10.3354/cr01262

Wang X, Pang G, Yang M, Wan G (2016a) Effects of modified soil water-heat physics on RegCM4 simulations of climate over the Tibetan Plateau. J Geophys Res Atmos 121:6692–6712. https://doi.org/10.1002/2015JD024407

Wang ZQ, Duan AM, Li MS, He B (2016b) Influences of thermal forcing over the slope/platform of the Tibetan Plateau on Asian summer monsoon: numerical studies with the WRF model. Chin J Geophys 59:3175–3187. https://doi.org/10.6038/cjg20160904

Wang X, Yang T, Wortmann M, Shi P, Hattermann F, Lobanova A, Aich V (2017) Analysis of multi-dimensional hydrological alterations under climate change for four major river basins in different climate zones. Clim Change 141:483–498. https://doi.org/10.1007/s10584-016-1843-6

Wang X, Yang T, Yong B, Krysanova V, Shi P, Li Z, Zhou X (2018) Impacts of climate change on flow regime and sequential threats to riverine ecosystem in the source region of the Yellow River. Environ Earth Sci 77:465. https://doi.org/10.1007/s12665-018-7628-7

Wang X, Yang T, Xu C, Yong B, Shi P (2019a) Understanding the discharge regime of a glacierized alpine catchment in the Tianshan Mountains using an improved HBV-D hydrological model. Glob Planet Change 172:211–222. https://doi.org/10.1016/j.gloplacha.2018.09.017

Wang Z, Ye A, Wang L, Liu K, Cheng L (2019b) Spatial and temporal characteristics of reference evapotranspiration and its climatic driving factors over China from 1979–2015. Agric Water Manag 213:1096–1108. https://doi.org/10.1016/j.agwat.2018.12.006

Xie Z, Hu Z, Gu L, Sun G, Du Y, Yan X (2017) Meteorological forcing datasets for blowing snow modeling on the Tibetan Plateau: evaluation and intercomparison. J Hydrometeorol 18:2761–2780. https://doi.org/10.1175/JHM-D-17-0075.1

Xu CY, Widen E, Halldin S (2005) Modelling hydrological consequences of climate change-progress and challenges. Adv Atmos Sci 22:789–797. https://doi.org/10.1007/BF02918679

Xu ZX, Gong TL, Li JY (2008) Decadal trend of climate in the Tibetan Plateau—regional temperature and precipitation. Hydrol Process 22:3056–3065. https://doi.org/10.1002/hyp.6892

Xu J et al (2018) On the role of horizontal resolution over the Tibetan Plateau in the REMO regional climate model. Clim Dyn 51:4525–4542. https://doi.org/10.1007/s00382-018-4085-7

Xue B et al (2013) Modeling the land surface water and energy cycles of a mesoscale watershed in the central Tibetan Plateau during summer with a distributed hydrological model. J Geophys Res Atmos 118:8857–8868. https://doi.org/10.1002/jgrd.50696

Yang K, He J, Tang W, Qin J, Cheng CCK (2010a) On downward shortwave and longwave radiations over high altitude regions: observation and modeling in the Tibetan Plateau. Agric Forest Meteorol 150:38–46. https://doi.org/10.1016/j.agrformet.2009.08.004

Yang MX, Nelson FE, Shiklomanov NI, Guo DL, Wan GN (2010b) Permafrost degradation and its environmental effects on the Tibetan Plateau: a review of recent research. Earth Sci Rev 103:31–44. https://doi.org/10.1016/j.earscirev.2010.07.002

Yang K, Wu H, Qin J, Lin C, Tang W, Chen Y (2014) Recent climate changes over the Tibetan Plateau and their impacts on energy and water cycle: a review. Glob Planet Change 112:79–91. https://doi.org/10.1016/j.gloplacha.2013.12.001

Yao T et al (2012) Different glacier status with atmospheric circulations in Tibetan Plateau and surroundings. Nat Clim Change 2:663–667. https://doi.org/10.1038/nclimate1580

Yao T et al (2019) Recent Third Pole's rapid warming accompanies cryospheric melt and water cycle intensification and interactions between monsoon and environment: multi-disciplinary approach with observation, modeling and analysis. Bull Am Meteorol Soc 100:423–444. https://doi.org/10.1175/BAMS-D-17-0057.1

You Q, Kang S, Wu Y, Yan Y (2007) Climate change over the Yarlung Zangbo River Basin during 1961–2005. J Geogr Sci 17:409–420. https://doi.org/10.1007/s11442-007-0409-y

You Q, Wang D, Jiang Z, Kang S (2017) Diurnal temperature range in CMIP5 models and observations on the Tibetan Plateau. Q J R Meteorol Soc 143:1978–1989. https://doi.org/10.1002/qj.3057

You Q, Jiang Z, Wang D, Pepin N, Kang S (2018) Simulation of temperature extremes in the Tibetan Plateau from CMIP5 models and comparison with gridded observations. Clim Dyn 51:355–369. https://doi.org/10.1007/s00382-017-3928-y

Yu Z, Gu H, Wang J, Xia J, Lu B (2018) Effect of projected climate change on the hydrological regime of the Yangtze River Basin, China. Stoch Environ Res Risk Assess 32:1–16. https://doi.org/10.1007/s00477-017-1391-2

Yuan F, Berndtsson R, Zhang L, Uvo CB, Hao Z, Wang X, Yasuda H (2015) Hydro climatic trend and periodicity for the source region of the Yellow River. J Hydrol Eng 20:5015003. https://doi.org/10.1061/(ASCE)HE.1943-5584.0001182

Zeng X, Zhao M, Dickinson RE (1998) Intercomparison of bulk aerodynamic algorithms for the computation of sea surface fluxes using TOGA COARE and TAO data. J Clim 11:2628–2644. https://doi.org/10.1175/1520-0442(1998)011%3c2628:IOBAAF%3e2.0.CO;2

Zhang S, Lü S, Bao Y, Ma D (2015) Sensitivity of precipitation over China to different cumulus parameterization schemes

in RegCM4. J Meteorol Res PRC 29:119–131. https://doi.org/10.1007/s13351-014-4042-2

Zhang X, Chen D, Yao T (2018) Evaluation of circulation-type classifications with respect to temperature and precipitation variations in the central and eastern Tibetan Plateau. Int J Climatol. https://doi.org/10.1002/joc.5708

Ziegler AD, Maurer EP, Sheffield J, Nijssen B, Wood EF, Lettenmaier DP (2005) Detection time for plausible changes in annual precipitation, evapotranspiration, and streamflow in three Mississippi River sub-basins. Clim Change 72:17–36. https://doi.org/10.1007/s10584-005-5379-4